

1 Polygenic basis of Bt Cry resistance evolution in wild *Helicoverpa zea*
2
3

4 **Authors:**

5
6 Katherine L Taylor¹, Jane Quackenbush¹, Cara Lamberty¹, Kelly A Hamby¹ & Megan L Fritz^{1*}
7

8 ¹ Department of Entomology, University of Maryland, College Park MD 20742
9

10 *Corresponding author

11 Email: mfritz13@umd.edu
12

13 **Keywords:**

14 *Helicoverpa zea*, *Bacillus thuringiensis*, Cry toxin, resistance evolution, gene amplification,
15 structural variant, trypsin, polygenic adaptation
16

17 **Short title:** Polygenic Bt resistance in *Helicoverpa zea*
18
19
20
21
22
23
24
25
26
27
28
29

30 **Abstract**

31 Strong and shifting selective pressures of the anthropocene are rapidly shaping phenomes
32 and genomes of organisms worldwide. One major selective force on insect genomes is crops
33 expressing pesticidal proteins from *Bacillus thuringiensis* (Bt). Here we characterize a rapid
34 response to selection by Bt crops in a major crop pest, *Helicoverpa zea*. We reveal the polygenic
35 architecture of Bt resistance evolution in *H. zea* and identify multiple genomic regions
36 underlying this trait. In the genomic region of largest effect, we identified a gene cluster
37 amplification, where resistant individuals showed variation in copy number for multiple genes.
38 Signals of this amplification increased over time, consistent with the history of field-evolved Bt
39 resistance evolution. Modern wild populations from disparate geographical regions are positive
40 for this variant at high, but not fixed, allele frequencies. We also detected selection against single
41 copy variants at this locus in wild *H. zea* collected from Bt expressing plants, further supporting
42 its role in resistance. Seven trypsin genes were present in this genomic region and all appeared
43 to be significantly upregulated in Bt resistant *H. zea*. Biochemically inhibiting trypsin activity
44 decreased *H. zea*'s tolerance to Bt. These findings characterize rapid genome evolution in a
45 major crop pest following anthropogenic selection and highlight the role that gene copy number
46 variants can have in rapid evolutionary responses.

47

48

49

50

51

52

53

54

55 **Introduction**

56 The study of evolution in the Anthropocene has revealed that adaptive organismal
57 responses can occur on timescales much shorter than previously thought possible (Carroll et al.
58 2007). Human activities impose strong and shifting selection pressure on communities of
59 organisms, shaping their phenomes and genomes (Palumbi, 2001). Empirical evidence of rapid
60 evolutionary change is mounting (e.g. Bergland et al., 2014; Bi et al., 2019; Campbell-Staton et
61 al., 2017; Chaturvedi et al., 2021; Ergon et al., 2019; Mikheyev et al., 2015; Roberts Kingman et
62 al., 2021; Rudman et al., 2022; Schiebelhut et al., 2018; Stahlke et al., 2021; Storz & Wheat,
63 2010), and has linked the strength and nature of selection to specific genomic variants that
64 enhance the fitness of wild organisms. Rapid evolution can result from allele frequency changes
65 at a single major effect locus, or at many loci across the genome (reviewed in Bay et al., 2017).
66 Currently, a major objective of the field of evolutionary genomics is to move beyond
67 documenting the phenomenon of rapid evolution, and instead, uncover the rules that govern how
68 these responses occur on short timescales. This includes characterizing the types of genomic
69 variants (*i.e.* single nucleotide polymorphisms, insertion/deletion polymorphisms, copy number
70 variants, epigenetic modifications) that are most critical for and facilitate rapid evolutionary
71 responses. Perhaps even more important is understanding how fitness-conferring variants came
72 to be; whether they arose *de novo*, were introduced through migration, or were selected from
73 standing genetic variation.

74 Agricultural ecosystems (agroecosystems) are useful for investigating mechanisms of
75 rapid evolution, both due to the well-understood nature of selection in these ecosystems and their
76 relatively simplified ecosystem structure (Chen & Schoville, 2018). One common feature of
77 agroecosystems is the use of population suppression practices, which exert strong pressure on so-
78 called agricultural pests to evade management through resistance evolution. High levels of

79 resistance can evolve rapidly (Brevik et al., 2018), and in arthropods alone, resistance to over
80 300 pesticidal compounds in more than 600 species has been documented (Fritz, 2022; Mota-
81 Sanchez & Wise, 2022). Rapid pesticide resistance evolution also has economic and
82 environmental consequences, which provides incentive for its study. Resistance evolution
83 causes billions of dollars in crop losses every year, and often results in increased environmental
84 pesticide inputs in an attempt to prevent these losses (Gould et al., 2018; Palumbi, 2001).

85 We have adopted the Bt cropping system as an experimental model for the study of rapid
86 organismal evolution. Since 1996, Bt crops have provided area-wide pest suppression, while
87 decreasing reliance on harmful broad-spectrum pesticides (Cattaneo et al., 2006; Dively et al.,
88 2018; Hutchison et al., 2010; Kathage & Qaim, 2012; Perry et al., 2016). Bt crops have been
89 engineered to express genes from the bacterium, *Bacillus thuringiensis*, which encode crystalline
90 (Cry) and vegetative insecticidal proteins (Vip). The proteins specifically target lepidopteran
91 and coleopteran species that damage crops, some of which have been historically challenging to
92 manage with sprayable, synthetic pesticides. They have been widely adopted for insect
93 management around the globe, and at present, 85% of corn and 89% of cotton planted in the
94 United States express Bt traits (USDA-ERS, 2023). Bt crops are, therefore, a major selective
95 force in agroecosystems (Gassmann & Reisig, 2023; Tabashnik & Carrière, 2017).

96 To improve the durability of these crops and slow resistance evolution, management
97 plans strongly rooted in evolutionary theory, modeling-based studies, and past empirical
98 observations were developed (e.g. Alstad & Andow, 1995; Frutos et al., 1999; Gould et al., 2018;
99 McGaughey et al., 1998). Bt crops were designed to produce a “high dose”, or 25 times the
100 amount of pesticidal protein needed to cause mortality in susceptible target pests (US EPA-SRP,
101 1998). Such a high dose was predicted to favor resistance arising from a single mutation of

102 major effect, rather than from standing genetic variation across the genome (McKenzie &
103 Batterham, 1994). Multiple toxins were also pyramided into Bt crops to redundantly kill pests
104 that evolved resistance to a single protein. Finally, non-expressing plants, or a “refuge” planted
105 nearby, should produce homozygous susceptible pests that dilute resistance alleles in a local
106 landscape (Gould, 1998; Huang et al., 2011). Under these circumstances, if resistance was
107 recessive and resistance alleles incurred a fitness cost in the absence of these toxic proteins, the
108 emergence and spread of resistance may be preventable (Gould, 1998). Although there have
109 been cases of successful resistance management in some target pests of Bt crops, practical
110 resistance has emerged in several lepidopteran and coleopteran species, including the
111 polyphagous pest, *Helicoverpa zea* (Tabashnik & Carrière, 2017).

112 *H. zea*, a pest of corn and cotton, was successfully managed by Bt crops when they were
113 commercially released in 1996. Yet within 20 years, susceptibility to Cry proteins in *H. zea* had
114 decreased and crop damage increased (Dively et al., 2016; Dively et al., 2023; Kaur et al., 2019;
115 Yang et al., 2019; Yang et al., 2022). Resistance evolution in *H. zea* had been predicted because
116 Cry expressing Bt crops do not produce a “high” dose for *H. zea* (Horner et al., 2003), and refuge
117 implementation for corn and cotton was often insufficient (Reisig, 2017; Reisig & Kurtz, 2018).
118 Resistance may also have been facilitated by cross pollination between Bt and refuge corn,
119 which produces kernels expressing low Cry toxin doses (Pezzini et al., 2024; Dively et al., 2020;
120 Yang et al., 2015). The Cry resistance that emerged in wild *H. zea* has provided an opportunity
121 to empirically examine the mechanisms underlying rapid adaptation in this human-altered
122 system. If *H. zea*’s Cry toxin exposure was not high dose and the strength of selection allowed
123 for survivors within their natural viability distribution, adaptive responses should have a
124 polygenic trait architecture (McKenzie & Batterham, 1994). Our previous work supported this

125 prediction, using two single-family QTL analyses to characterize the molecular architecture of
126 resistance to two separate Bt crop cultivars (Taylor et al., 2021).

127 Cry toxicity is generally understood to begin with solubilization and activation of the Cry
128 protoxin by proteolytic enzymes in the insect digestive system, although this activation step is
129 not necessary for the activated toxins expressed by many Bt crops (Clark et al., 2005; Gould,
130 1998; Székács et al., 2010). Activated toxins interact with a series of midgut receptors,
131 eventually causing lysis of the midgut epithelial cells and leading to growth suppression or
132 mortality in targeted insects (Heckel, 2020; Jurat-Fuentes et al., 2021; L. Liu et al., 2021). The
133 multi-step and complex molecular mechanism of Cry toxicity provides many molecular and
134 physiological pathways for the evolution of resistance. In other lepidopteran species, resistance
135 has generally been connected to the disruption of the midgut toxin binding sites or reduced
136 expression of target genes, although there are also examples of resistance associated with altered
137 Bt protein processing, detoxification, and changes in immune function (Heckel, 2020; Jurat-
138 Fuentes et al., 2021; L. Liu et al., 2021). Our prior work with *H. zea* led us to reject most of the
139 common Cry resistance mechanisms described in other lepidopteran species, and instead pointed
140 to novel resistance-related genomic regions (Taylor et al., 2021), with one under particularly
141 strong selection by Cry toxins (Pezzini et al. 2024).

142 Here, we have expanded our analysis of the rapid adaptation to Bt crops observed in wild
143 *H. zea*, describing its underlying genetic architecture. We provide further evidence to support a
144 polygenic trait architecture of Cry resistance in wild *H. zea*. We also provide the first evidence
145 that a copy number variant (CNV) containing a cluster of 10 genes plays a major role in the Cry
146 resistance phenotype we observed in *H. zea*. Our results connect the introduction and adoption
147 of transgenic crops in the landscape, which resulted in a resistance phenotype, to genomic targets

148 of selection, and the nature of the genomic variants that facilitated *H. zea*'s rapid evolutionary
149 response.

150 **Results**

151 **Cry resistance and general growth phenotypes**

152 To link regions of the *H. zea* genome to Cry resistance phenotypes, we used a replicated
153 quantitative trait locus (QTL) analysis. This well-established approach relies on crosses between
154 individuals from phenotypically distinct inbred lines or outbred populations to produce F₂
155 offspring, whose chromosomes represent unique genomic combinations from cross founders
156 (Falconer, 1996; Lynch & Walsh, 1998). Correlated traits within phenotypically distinct cross-
157 founding populations are, therefore, uncorrelated in F₂ progeny due to genome-wide
158 recombination during meiosis. We crossed field-evolved resistant grandparents to one of very
159 few known susceptible *H. zea* populations in our replicated design. This allowed us to test for
160 genome-wide associations between field-relevant Cry resistance phenotypes and genotypes
161 across recombined F₂ chromosomes. While multiple genomic regions were associated with Cry
162 resistance in our previous work (Taylor et al. 2021), testing of additional replicate families
163 increased our power to detect loci of major effect that commonly contribute to field-evolved Cry
164 resistance in wild *H. zea*.

165 We initially measured Cry resistance phenotypes for a field resistant population and a
166 long-term laboratory-reared susceptible population, as well as the F₂ hybrid offspring from 10
167 intercross families. Resistant individuals should be able to grow while feeding on diets
168 containing Cry toxins, though at different rates depending on the number and effect size of their
169 Cry resistance alleles, while susceptible individuals should not. Thus, measuring weight

170 following 7 days exposure to Cry toxin-incorporated diet served as our metric of resistance. A
171 critical component of our experimental design included measurement of intra-family controls,
172 where half of the offspring from each cross were assayed on identical diets lacking Cry toxin.
173 These intra-family controls served as a way to measure and, if necessary, exclude general
174 growth-related QTL as candidates for resistance. If a QTL were truly related to Cry resistance,
175 we reasoned that QTL associated with growth on Cry toxin-incorporated diet in one half of the
176 family should not overlap with QTL for general growth in their siblings reared on a diet lacking
177 Cry toxins. Therefore, larvae from each family were exposed to diets containing either a
178 diagnostic dose of Cry1Ab or Cry1A.105 + Cry2Ab2 expressing corn leaf tissue and leaf tissue
179 from the non-expressing corn near isolines, as described in Dively et al. (2016) and Taylor et al.
180 (2021) (**Figure 1, Figure S1, Table S1, Table S2**).

181 The larval population from which resistant cross-founding grandparents were drawn
182 grew significantly larger than laboratory-reared, susceptible larvae on both Cry1Ab and
183 Cry1A.105 + Cry2Ab2 expressing corn leaf tissue incorporated diets (**Figure 1, Table S1**). Yet
184 even in the absence of Cry toxins, the susceptible population grew significantly less than did the
185 resistant population, suggesting that growth on toxin and general growth were correlated in the
186 grandparental populations. This was likely a result of long-term reproductive isolation between
187 these populations resulting in substantial phenotypic and genomic divergence between them.
188 Growth phenotypes in the F₂ offspring suggested that resistance to all the Cry toxins we tested,
189 as well as growth on the control treatments were quantitative genetic traits (**SI Results**). Based
190 on our experimental design, we predicted that recombination in the F₁ generation should reduce
191 correlations between growth on control and toxin-incorporated diet within individual F₂

192 offspring, resulting in limited overlap between general growth and Cry resistance QTLs
193 discovered in our assays.

194 **Marker generation and variant calling**

195 Grandparents, parents, and progeny from 10 replicated intercross families were
196 sequenced on an Illumina NovaSeq 6000. Whole genome sequencing (WGS) of the 20 cross
197 parents resulted in a total of 4,716,009 high quality genome wide single nucleotide
198 polymorphisms (SNPs) following read filter-trimming and alignment to the *H. zea* genome (v.
199 1.0, PRJNA767434; Benowitz et al., 2022). Genome wide average sequencing coverage of
200 18.6 \times (st. dev. = 2.4) ensured accuracy of the genotyping calls. Divergence between the field
201 collected resistant and laboratory susceptible founding populations was high genome wide
202 (**Figures S2 & 3, SI Results**), as would be expected due to the long-term sexual isolation
203 between them.

204 Double digest restriction site associated DNA (ddRAD) sequencing of F₂ offspring
205 resulted in 78,580 - 79,408 high quality SNP markers for genotype-phenotype association in
206 each treatment. Final SNP marker numbers likely varied because of true differences in SNP
207 presence, different loci passing quality control filters, and genetic variation among individuals at
208 restriction cut sites used for marker development (Davey et al., 2013). The average sequencing
209 coverage per ddRAD locus across all F₂s was 52,225 \times (st. dev. = 45,011), and the average
210 coverage per locus per individual was 63 \times . SNPs were further filtered to include only those
211 variants where the allele origin population (field resistant vs. lab susceptible) could be reliably
212 predicted to determine their directional effect on growth. This produced the smaller filtered sets
213 of 6,717 - 6,749 genome wide SNPs for each treatment that were used for visualization of effect
214 size and direction.

215

216 **Polygenic Cry resistance architecture**

217 To link ddRAD marker genotypes with Cry resistance phenotypes, we used gemma
218 (Zhou et al., 2013). This software estimates both the number of loci underlying complex traits
219 (including those of small effect size), as well as the impact of each large effect locus on a trait,
220 while accounting for the relatedness among individuals in a test population. A significant
221 proportion of phenotypic variation (PVE) in the F₂ offspring could be explained by the full set of
222 ddRAD markers. Mean PVE estimates were 69.7% [95% CI = 45.4 - 93.7] for the Cry1Ab
223 treatment and 71.1% [95% CI = 43.6 - 96.5] for the Cry1A.105 + Cry2Ab2 toxin blend, and
224 lower for the control growth treatments 44.7% [95% CI = 20.3 - 71.9] and 51.2% [95% CI = 27.1
225 - 74.1] (**Figure S4**).

226 The numbers of variants predicted to have large effect sizes on growth were similar
227 across treatments, with mean estimates ranging from 11.3 - 34.1, further supporting a polygenic
228 trait architecture. In all cases, there were wide overlapping credible intervals around these
229 means, suggesting that tens of genomic variants of major effect underlie phenotypic differences
230 in all growth-related traits (**Figure S4**). Large effect size variants contributed to 74.0% [95% CI
231 = 36.9 - 98.6] of the Cry1Ab growth-related variance explained by our full marker panel (PGE).
232 For the Cry1A.105 + Cry2Ab2 treatment, 77.8% [95% CI = 46.8 - 98.9] of the growth-related
233 variance could be explained by variants of large effect size. These values dropped to 53.4%
234 [95% CI = 0.5 - 97.3%] and 73.6% [95% CI = 24 - 99.2] for the control treatments (**Figure S4**).
235 Notably, the high PVE and PGE estimates for both Cry treatments suggest that our data captured
236 much of the genetic basis of field evolved resistance in *H. zea*.

237 **Genomic regions underlying Bt Cry resistance**

238 To identify the chromosomal regions underlying field evolved Cry resistance, we
239 estimated the additive effect (β) of a single resistant cross-founder allele on 7 day weight in mg.
240 Smoothed additive effects of genome-wide markers on growth are shown for Cry1Ab,
241 Cry1A.105 + Cry2Ab2, and control treatments in **Figure 2**. The major effect QTL revealed in
242 Figure 2 were also identified using multiple SNP filtering criteria and in the unsmoothed data set
243 (**Figures S5 & 6**), indicating that our detection of major effect QTL is robust to differences in
244 bioinformatic and analytical approaches. A resistant parent allele in F_2 offspring significantly
245 and strongly increased growth on Cry1Ab in regions of Chromosomes (Chr) 2, 3, 6, 9, and 30
246 with a significance threshold of Bonferroni corrected $p < 0.01$ (**Figure 2A**). With the less
247 stringent criteria of Bonferroni corrected $p < 0.05$ we also detected an association of parts of Chr
248 11 and 21 (**Figure 2A**). For Cry1A.105 + Cry2Ab2, we only detected a significant effect of Chr
249 9, though non-significant peaks suggest possible shared QTL with the Cry1Ab treatment on Chr
250 2 and 30 (**Figure 2C**). We detected genomic regions associated with general growth in the
251 laboratory assays on Chr 10, 14 and 27 (**Figure 2B**). As predicted for F_2 offspring, we observed
252 little overlap between QTL underlying growth on toxin-containing and control treatments. Chr
253 10 was the only Chr with a major effect on growth on both control and toxin-containing
254 (Cry1Ab) treatments (**Figures 2A & B**). Therefore, we did not consider this region to be Cry
255 resistance related. The negative direction of this effect also suggested that the growth associated
256 allele on Chr 10 is more common in the susceptible parent population. Notably, we did not
257 detect any fitness cost of Cry resistance-associated genomic regions, which would have appeared
258 as negative values for these variants in the subsets of F_2 s on non-Cry expressing treatments
259 (**Figures 2B & D**).

260 The region of the genome with the largest additive effect on resistance was on Chr 9 for
261 both Cry-containing treatments (**Figures 2A & C**). There was no signal of an effect of Chr 9 on
262 general growth, however (**Figures 2B & D**). For individuals grown on the Cry1Ab treatment, we
263 identified a clear peak between 5 and 6 Mb on Chr 9. This aligned well with previously
264 identified signals of genomic divergence over time at 5.75 Mb on Chr 9 in wild *H. zea* (Taylor et
265 al. 2021). We also identified a directly overlapping divergence peak at 5.75 Mb between
266 resistant and susceptible cross founders (SI Results). Between 5 and 6 Mb on Chr 9, there were
267 45 genome annotations (**Table S3**), several of which we examined further (see below). The QTL
268 on Chr 30 had clear peaks at ~2.5 and ~3.3 Mb, making it possible to describe nearby gene
269 candidates for the Cry resistance observed in our study. Within 100 Kb of those Chr 30
270 association peaks (2.4 - 3.4 Mb) were a MAP kinase-activated protein kinase 2-like,
271 *HzeaTryp129*, and *HzeaABCC11*, toll-like receptors, a cluster of carboxylesterases, and
272 carboxylase-like genes (**Table S4**), suggesting that several known Bt candidate gene families and
273 insecticide resistance related genes could underlie this QTL. The other identified QTL on Chr 2,
274 3 and 6 had more diffuse genomic signals with less well-defined peaks, making it difficult to
275 identify narrow regions most linked to resistance. In the SI Results, we further describe the
276 limited evidence for any role of other major candidate genes.

277 **Resistance-associated differential gene expression**

278 We paired our QTL study with differential gene expression analyses to narrow in on
279 potential targets of selection. The mechanism of Cry toxin action takes place in the larval
280 midgut, and changes in gene expression in this tissue have strong potential to impact resistance.
281 Therefore, we initially focused on differential midgut gene expression between wild, resistant *H.*
282 *zea* larvae collected directly from Cry1A.105+Cry2Ab2-expressing corn and laboratory-reared,

283 susceptible larvae. Of the 14,600 annotated genes, 527 genes were significantly upregulated and
284 352 were significantly downregulated in the population collected from Cry expressing corn
285 relative to the susceptible population (p-adjusted < 0.01; **Table S5**). Of those significantly
286 differentially expressed genes, 33 were within 100 kb of at least one SNP significantly associated
287 with resistance to Cry1Ab, Cry1A.105 + Cry2Ab2, or both treatments (**Table S6**). This analysis
288 identified several significantly upregulated genes in resistant larvae that were found near QTL,
289 signaling their potential involvement in resistance. One was an aminopeptidase gene found on
290 Chr 9 (*apn1*) (**Table S6**). *apn1* is a known Cry resistance candidate gene, for which reduction of
291 expression increases Cry resistance (Herrero et al., 2005; X. Ma et al., 2022; Sun et al., 2022). In
292 our work, however, *apn1* expression increased in our resistant population, which was
293 inconsistent with its previously described role in resistance. The most striking gene expression
294 differences were found among seven significantly upregulated trypsin genes arranged in tandem
295 between 5 and 6 Mb in the Chr 9 QTL. Six of these trypsins in the tandem array on Chr 9 were
296 among the top 50 most differentially expressed genes genome wide (**Figure 3B, Table S5**).

297 Trans-acting factors also impact regulation of gene expression, which would result in
298 separation of differentially expressed genes from QTL. When we considered only our
299 differential gene expression analysis, six other trypsins spread across multiple chromosomes
300 were also among the top 50 most differentially expressed genes (**Table S5**). Several other
301 insecticide resistance candidate gene families also had members among the top 50 most
302 differentially expressed genes, including, a cadherin-87A-like gene and a cytochrome P450
303 (CYP301B1), both of which were downregulated in resistant individuals (**Table S5**).

304 We also tested for Cry inducible gene expression changes between wild *H. zea* larvae
305 collected from Cry expressing and non-expressing corn. A comparison of midgut gene

306 expression for these groups revealed that expression of a small number of genes was modulated
307 by Cry toxin exposure. Thirteen genes were significantly upregulated and 20 genes significantly
308 downregulated in larvae collected from expressing corn (**Table S7**). Four trypsin and one
309 chymotrypsin were among the most upregulated genes in Cry exposed resistant individuals. Only
310 one of the trypsin found between 5 and 6 Mb on Chr 9, *tryp80*, was in this group showing Cry
311 inducible expression changes. Downregulated genes in Cry exposed individuals included a
312 cadherin-87A-like gene and the immune-related gene, Lysozyme1.

313 **A potential genetic mechanism of large effect on Bt Cry resistance**

314 Taken together, evidence from the QTL and differential expression analysis suggested
315 that a region of Chr 9 containing a cluster of differentially expressed genes, including 7 trypsin,
316 was strongly associated with Cry resistance (**Figures 3B & C**). Closer investigation of this
317 region revealed a structural variant from 5.22 - 5.37 Mb on Chr 9 (**Figure 4A**). In this region
318 encompassing the full cluster of differentially expressed genes, resistant cross founders had
319 increased whole genome sequencing depth of coverage relative to their genome wide average
320 (**Figure 4A**). Elevated coverage depth indicated this region of the genome was at least
321 duplicated in resistant cross founders. The observed upregulation of most genes in this gene
322 cluster in resistant individuals was consistent with a mutational event that duplicated the entire
323 gene cluster (**Figure 3B**).

324 To confirm that the coverage and differential expression signals we detected were truly
325 related to gene cluster duplication, we quantified the copy number variation for one
326 representative gene in the cluster (*tryp77*) using droplet digital polymerase chain reaction
327 (ddPCR) (**Figure 4B**). If *tryp77* existed as a single copy gene, our ddPCR results should reveal a
328 copy number equal to two in this diploid species. Instead, our analysis showed that all resistant

329 cross founders from our study had more than two copies of *tryp77*, while all susceptible founders
330 had the expected two copies. Variation in copy number existed among the field-collected
331 resistant individuals used in our analysis, indicating there is not a single allele, but multiple
332 alleles linked to resistance at this Chr 9 locus. There was a strong relationship between copy
333 number detected by ddPCR and relative coverage depth of the gene cluster ($r^2 = 0.95$), suggesting
334 that WGS coverage depth is a reasonable proxy measure for copy number.

335 We used publicly available WGS data from Taylor et al. (2021) and Pezzini et al. (2024)
336 to determine whether variation in copy number at this Chr 9 locus could also be found in other
337 wild North American *H. zea* populations. Increased depth of coverage was not found in WGS
338 data from the susceptible lab population or in field samples collected in 2002, decades before
339 Cry resistance was widespread (**Figures 4A-D**). Absence of this variant in samples collected in
340 2002 suggested that: 1) it may have arisen after 2002, 2) it existed as a rare allele at our study
341 site prior to 2002, or 3) it arose in or before 2002, but at a location not sampled for our work.

342 Analysis of WGS data from these *H. zea* samples collected from Louisiana in 2017
343 (**Figures 4C & D**), and North Carolina in 2019 (**Figures 4E & F**) revealed signals of increased
344 coverage depth in this Chr 9 region, similar to what we observed in the resistant cross founding
345 individuals collected from Maryland in 2019 and 2020 (**Figure 4A**). The presence of this
346 sequence duplication in samples collected across 3 separate regions of North America over
347 multiple years, suggests that this genetic variant is widespread. Notably, depth of coverage at
348 this locus increased over time, with increased coverage depth first appearing in 2012 and the
349 strength of that signal increasing in 2017 (**Figures 4C & D**).

350 In 109 samples collected from experimental plots in North Carolina in 2019, we detected
351 increased coverage depth in this Cry resistance-associated Chr 9 region in individuals collected

352 from Cry expressing plants compared to individuals collected from non-Bt plants in structured
353 and blended refuge plots (Structured refuge: $t = 2.61$, adjusted $p = 0.039$, Blended refuge: $t =$
354 2.67 , adjusted $p = 0.033$) (**Figure 4E & F**). The consistent difference in coverage depth between
355 the population collected on Cry expressing plants and both refuge conditions and suggests that
356 selection by the Cry expressing plants limited the growth and survival of individuals with lower
357 sequence duplication in this region, providing another line of evidence for the role of this genetic
358 variant in Cry resistance evolution. In these samples, we also observed a continued increase in
359 sequencing depth over time, with samples from 2019 and 2020 (**Figure 4A & E**) showing
360 stronger signals of this amplification than those from 2012 and 2017 (**Figure 4C**). This could
361 reflect increased numbers of individuals homozygous for a duplication or additional duplication
362 events. Though none of the resistant samples collected in MD and NC in 2019 and 2020 appear
363 to be single copy in this region (**Figure 4A & E & F**), some individuals collected from non-
364 expressing plants are (**Figure 4E & F**), indicating that this variant is likely at high frequency but
365 not fixed in modern populations. Samples collected in 2019 and 2020 also have markedly higher
366 coverage between 5.32 and 5.35 Mb, region contains *tryp79* and *tryp80*, relative to other parts of
367 the duplicated cluster and historical samples. We speculate that this particular region may have
368 undergone multiple duplication events.

369 The strong association of *tryp77* copy number and depth of WGS coverage motivated us
370 to analyze the correlation between ddRAD sequencing coverage depth and weight for the F_2
371 offspring from our experimental crosses (**Figure 4G**). We reasoned that F_2 individuals with
372 higher coverage at this locus should, on average, have higher weights than those with low
373 coverage, if copy number variation was involved in Cry resistance. Likewise, if increasing copy
374 number is only related to Cry resistance and not generally associated with weight gain, we

375 reasoned that any positive correlation between weight and coverage depth should be observed for
376 individuals fed on Cry-treated diet, but not for their siblings on untreated diet. Indeed, ddRAD-
377 seq coverage depth of the Chr 9 gene cluster was significantly higher for the F₂ offspring that
378 grew most on both toxin containing diets compared to the offspring which grew the least
379 (Cry1A.105 + Cry2Ab2: $t = 5.2054$, p adjusted < 0.001, Cry1Ab: $t = 3.4574$, p adjusted <0.001)
380 (**Figure 4G**). On both control diets, there was no relationship between relative coverage and
381 growth (Control 1: $t = -1.5115$, p = 0.1323, Control 2: $t = 0.46397$, p = 0.6432) (**Figure 4G**). As
382 this is a polygenic trait and the Chr 9 locus was not the only one to confer Cry resistance (**Figure**
383 **2A**), we expected that F₂ genotype at this locus would not perfectly predict phenotypes.
384 However, the strong association of ddRAD-seq coverage with resistance phenotype indicates that
385 the region containing this amplified gene cluster likely explains most of the association between
386 Chr 9 and Cry resistance.

387 **Synergistic effect of trypsin inhibition and a Cry toxin**

388 Ten genes were found in the region of copy number variation on Chr 9, and seven of
389 these genes encoded trypsins. To assess whether trypsins, including those on Chr 9, were
390 involved in Cry resistance, we inhibited their activity with N- α -tosyl-1-lysine chloromethyl
391 ketone (TLCK) in resistant and susceptible populations of *H. zea*. If trypsin activity, including
392 the activity of those on Chr 9, were involved in Cry resistance, we reasoned that their inhibition
393 should interfere with growth on Cry treated diet. Trypsins are generally involved in lepidopteran
394 metabolism (Muhlia-Almazán et al., 2008), and their inhibition could also lead to stunted growth
395 on untreated diet. Yet if the midgut expressed trypsins on Chr 9 had activity unique to Cry
396 resistance, we reasoned that increasing dosages of a trypsin inhibitor should more strongly
397 impact the weights of larvae feeding on Cry-treated diet, compared to those fed trypsin inhibitor

398 on an untreated control diet. This trend should be true for both susceptible individuals bearing
399 single copy genes in the cluster, as well as resistant individuals with copy number variation. We
400 solubilized TLCK in a phosphate saline buffer (PBS) to make different concentrations of trypsin
401 inhibitor, and each concentration was mixed with our leaf tissue-incorporated diets. Early
402 second instar larvae were grown on either a diagnostic diet of Cry1Ab expressing corn leaf tissue
403 or leaf tissue from the non-expressing near isoline, each with increasing dosages of TLCK.
404 Larval weight was examined after a 7 day diet exposure. We confirmed that incorporation of
405 PBS did not impact larval growth relative to our standard non-expressing leaf tissue diet ($p >$
406 0.05, data not shown), and therefore larval growth on buffer alone was used as a control for all
407 further analyses and visualization.

408 To understand the extent to which trypsin inhibition influenced Cry resistance, we
409 calculated a growth ratio, which compared growth on the Cry-treated and untreated diets at each
410 TLCK dose. If trypsins, including those in our Chr 9 cluster, showed no special activity related
411 to Cry resistance, we reasoned that the ratio of larval weights on these diet treatments should
412 remain constant with increasing doses of a trypsin inhibitor. Instead the growth ratio was
413 negatively correlated with TLCK dose, suggesting that increased suppression of trypsin activity
414 had a proportionally greater impact on the weights of larvae grown on Cry-treated diets, than
415 those on untreated diet (**Figure 5**). The interaction between TLCK dose and Cry1Ab exposure
416 on larval weight was statistically significant for both resistant and susceptible *H. zea* populations
417 ($p < 0.001$) (**Figure 5, Table S8**), and post hoc contrasts of the estimated marginal means
418 confirmed that a trypsin inhibitor paired with Cry1Ab toxin significantly decreased larval growth
419 (**Table S9**). Notably, the mean weight of larvae from the resistant population fed on the Cry1Ab
420 and 10X TLCK treatment was 17.4 mg, suggesting that strongly inhibiting trypsins in resistant

421 individuals could reduce their Cry tolerance to levels observed in the susceptible population
422 (mean = 20.7 mg; **Table S8**). These results failed to falsify a role for trypsin in Cry resistance,
423 including those from our Chr 9 copy number variant (CNV). Overall, our findings suggest that
424 trypsin activity serves as one protective mechanism against Cry1Ab toxin expressed in corn.

425 **Discussion**

426 Here, we confirm the polygenic nature of *H. zea*'s adaptation to transgenic crops in
427 agroecosystems, and we begin to shed light on the mechanisms underlying their rapid
428 evolutionary response. Using replicated, split-family QTL analyses, we identified multiple
429 genomic regions associated with Bt resistance, most of which are not shared by siblings that
430 grew well on untreated diets (**Figure 2**). This lack of overlap demonstrates that the multiple
431 genomic regions associated with growth on Cry-containing diets are Cry resistance loci.
432 Polygenic adaptation to Cry toxins was predicted for *H. zea* because selection by Bt crops was
433 expected to act within its broad phenotypic range of Cry tolerance values. Early studies of field-
434 collected *H. zea* described this range and documented that laboratory selection could rapidly
435 increase population-level Cry tolerance (Luttrell et al., 1999). Our data provide empirical support
436 for the prediction that polygenic adaptation is favored when selection acts on phenotypes within
437 the natural range of variation of a population (McKenzie and Batterham 1994).

438 Tens of loci contribute to the polygenic basis of Cry resistance in *H. zea*, but the genomic
439 region of largest effect on both Cry1Ab and Cry1A.105 + Cry2Ab2 resistance was found on Chr
440 9. All resistance associated genomic regions are likely to be important to the Cry tolerance
441 observed in wild *H. zea*, and other loci should be the focus of future investigations. It is likely
442 that genetic interactions among the Cry resistance loci revealed in our work are critical for
443 production of strong Cry resistance phenotypes, as is observed in other species (Ma et al. 2022,

444 Sun et al. 2022). However, much of our analyses focused on Chr 9, providing us with insight
445 into the nature of the genetic mutations that facilitated rapid evolution in this system. We used
446 multiple lines of evidence to document the nature of the Chr 9 locus and demonstrate its
447 importance to Cry1Ab resistance both in our lab-based QTL experiments, as well as in field-
448 collected populations.

449 For our first line of evidence, we showed that field-collected Cry resistant *H. zea*
450 overexpressed multiple genes in a 10 gene cluster situated within the Chr 9 genotype-phenotype
451 association peak (**Figure 3**). Changes in gene expression are well known to underlie adaptive
452 phenotypes, including for cases of rapid insecticide resistance evolution (Amezian et al., 2021;
453 Guo et al., 2021; Nauen et al., 2022; Wilding, 2018). An alternative explanation for increased
454 expression of an entire gene cluster is sequence duplication, however (Heckel, 2022;
455 Kondrashov, 2012). We used ddPCR of our cross-founding parents to demonstrate that field-
456 evolved Cry resistant *H. zea* currently carry multiple copies of at least one representative gene
457 (*tryp77*) in the cluster. From this, we concluded that a CNV found in the 5-6 Mb region of Chr 9
458 was strongly (but not exclusively) associated with field-evolved Cry resistance in *H. zea*. It was
459 not possible to reconstruct the full sequence of this large CNV with the short read sequencing
460 approaches used in this study, and future studies should employ long read sequencing to describe
461 haplotypic variation in this genomic region.

462 Our second line of evidence for the role of this region in Cry resistance was the change in
463 copy number variation on Chr 9 over time in wild *H. zea*. Changes in Cry1Ab and
464 Cry1A.105+Cry2Ab2 tolerance in wild *H. zea* slowly increased following commercialization of
465 Bt crops in 1996 (Dively et al. 2016). Early warning signs of resistance emerged in 2008
466 (Brévault et al., 2013) and widespread practical resistance to both Cry1A and Cry2A toxins was

467 documented by 2016 (Dively et al., 2016; Reisig et al., 2018; US-EPA, 2018; Yang et al., 2019).
468 Using WGS read coverage depth as a proxy for copy number, we documented an increase in
469 copy number at this locus in wild *H. zea* over time. Consistent with previous resistance
470 observations, *H. zea* collected from LA in 2002 showed no evidence of a CNV, those from 2012
471 showed evidence of a rare CNV, and most 2017 individuals carried the variant. This indicated
472 that the Chr 9 CNV was widespread by the time *H. zea* could readily feed on Cry-expressing
473 corn ears in the field.

474 Our recent collections of the cross-founding parents from MD in 2019 and 2020 showed
475 that the Chr 9 CNV was not fixed for a specific copy number. While all resistant cross founders
476 carried a Chr 9 CNV, some carried different numbers of copies (**Figure 4B**), which likely confer
477 different levels of fitness under selection pressure by Cry toxins. This idea motivated the
478 analysis which provides a third line of evidence for the involvement of the Chr 9 CNV in *H.*
479 *zea*'s rapid adaptation to Bt crops. A re-analysis of WGS data from wild *H. zea* collected as part
480 of a field experiment in NC in 2019-2020 (Pezzini et al. 2024) documented that the Chr 9 locus
481 continues to be under strong selection by Cry toxins. Larvae collected directly from
482 Cry1Ab+Cry1F expressing field corn showed significantly greater WGS coverage depth of this
483 loci, our proxy for copy number variation, than did individuals collected from structured or
484 blended refuge ears (**Figures 4E & F**). We previously showed that SNPs in this CNV-
485 containing region were under strong Cry selection (Pezzini et al. 2024), but here we
486 demonstrated that a generation of selection by Cry1Ab+Cry1F increased the copy number in
487 wild *H. zea*. Moreover, coverage signals suggested that no individuals collected from
488 Cry1Ab+Cry1F expressing corn had single copy genotypes, while their conspecifics collected
489 from non-expressing corn in the same small experimental plots did. These data suggest that the

490 CNV on Chr 9 continues to be under selection for increased copy number, even though copy
491 number variation is widespread in the North American landscape.

492 Interestingly, seven of the ten genes within the CNV were trypsins, all of which were
493 differentially expressed (**Figure 3B**). The highest WGS coverage depth in wild *H. zea* collected
494 on Cry1Ab+Cry1F expressing corn in NC also spanned two of those trypsins. Moreover,
495 expression of one of the trypsin genes within this cluster, *tryp80*, appeared to be inducible upon
496 exposure to Cry-expressing corn (**Table S7**). Trypsins are a gene family previously thought to
497 be involved in lepidopteran Cry resistance via toxin activation or degradation (Gong et al., 2020;
498 González-Cabrera et al., 2013; C. Liu et al., 2014; Y. Ma et al., 2013). We demonstrated that
499 trypsin inhibition synergistically reduced growth in Cry containing treatments for both resistant
500 and susceptible populations. These findings demonstrated a significant protective effect of
501 trypsin activity in Cry exposed *H. zea*. When exposed to the highest TLCK dose and Cry toxin
502 together, growth in the resistant population was suppressed to the level of the susceptible
503 population on Cry toxin alone. The shared response of susceptible and resistant populations to
504 TLCK in this assay suggests that the increased expression and duplication of trypsins might
505 allow the resistant population to better utilize a mechanism already present in the susceptible
506 population.

507 Previous work has also linked trypsin activity to Cry resistance in *H. zea*, for example,
508 Lawrie et al. (2020) found strong signals of trypsin upregulation in resistant *H. zea* while Zhang
509 et al. (2019) found that trypsin down regulation was related to *H. zea* Cry resistance in a
510 laboratory selected line. The upregulation of trypsins in resistant individuals observed here
511 suggests degradation rather than activation as the potential mechanism for these genes'
512 involvement in resistance. This would be expected in the case of resistance to crops that express

513 activated toxin. Phenotypic resistance due to Cry toxin degradation by trypsin has been reported
514 in field populations of *Spodoptera exigua* (Y. Ma et al., 2013). Our findings along with results
515 from other Lepidoptera suggest a potential resistance mechanism: gene amplification causes
516 increased expression of these trypsin which, in turn, may degrade activated Cry toxins.

517 The CNV on Chr 9, likely plays an important role in resistance, but we emphasize that it
518 is not the only region involved in *H. zea*'s rapid adaptation to Bt crops. We also identified
519 resistance associated genomic regions on Chr 2, 3, 6, and 30. Multiple promising candidate genes
520 were found in the QTL peak on Chr 30 and near other QTL. There were also multiple candidate
521 Bt resistance genes among the top differentially expressed genes between resistant and
522 susceptible *H. zea*, including a cadherin gene. The genomic architecture of Bt resistance likely
523 involves interactions between some of these candidates of large to moderate effect size, as well
524 as undetected small effect size loci to produce the resistance observed in wild *H. zea*. Indeed,
525 our results showed that, on average, large Cry-exposed F₂s had significantly higher depth of
526 sequencing coverage, and therefore copy number in our Chr 9 CNV, than did smaller Cry-
527 exposed F₂s (**Figure 4G**). However, some small F₂s contained the Chr 9 CNV, while some large
528 F₂s did not. As expected based on the multiple QTL regions uncovered in our analysis, this
529 suggests one or more additional segregating resistance alleles are additively or synergistically
530 interacting with the Chr 9 CNV to produce resistance phenotypes. Consistent with our findings,
531 interactions between mutations in multiple genes have been described in laboratory studies of
532 other lepidopteran species (Ma et al. 2022, Sun et al. 2022). Further experimental work targeting
533 the Cry resistance associated regions on Chr 2, 3, 6 and 30 will be necessary to identify the
534 additional mutations underlying field-evolved Cry resistance.

535 In our non-expressing control growth treatments, we did not detect any fitness costs of
536 this Cry resistance associated gene amplification, or any of the other detected major effect loci
537 (**Figure 2**). The lack of fitness cost for resistance, the low dose of the toxins, incomplete refuge
538 implementation, and cross pollination, likely contributed together to the failure of Cry resistance
539 management strategies for *H. zea*. A degradation mechanism for toxin resistance could explain
540 the rapid evolution of resistance to multiple toxins that do not share binding sites. Our findings
541 link the same gene amplification to resistance to both Cry1Ab and blends of Cry1A.105 +
542 Cry2Ab2 and Cry1Ab+Cry1F. It may also be associated with resistance to other Cry toxins not
543 tested here. If, as our results suggest, trypsin activity underlies Bt resistance phenotypes in field
544 *H. zea* populations, then targeted synergist trypsin inhibitors could potentially be developed to
545 restore efficacy of Bt crops in controlling *H. zea* (Correy et al., 2019).

546 Gene duplications, an important source of genetic variation for phenotypic evolution,
547 have been linked to many cases of insecticide and herbicide resistance evolution (Bass & Field,
548 2011; Heckel, 2022). Duplications of detoxification related genes can immediately confer
549 resistance by increasing the quantity of already functional detoxification enzymes or can
550 additionally lead to new mechanisms of resistance by neofunctionalization. Multiple cases of
551 insecticide resistance have been functionally linked to new duplications of cytochrome P450s
552 and carboxylesterases, two detoxification related gene families (Bass et al., 2013; Cattel et al.,
553 2021; Mouches et al., 1990; Puinean et al., 2010; Schmidt et al., 2010). Our findings here
554 suggest a new example of the duplication of a detoxification related gene leading to insecticide
555 resistance, and the first case of this mechanism linked to Bt resistance. It is possible that gene
556 duplication may be more likely to underlie rapid phenotypic evolution than other variant types,
557 but the prevalence of structural variants is not well described as detection is difficult with current

558 technologies (Ho et al., 2020; Mahmoud et al., 2019). As gene amplifications have frequently
559 been linked to resistance evolution, genomic monitoring for resistance should be extended to
560 consider a range of genomic variant types beyond SNPs (Fritz 2022).

561 **Methods**

562 **Insect samples and phenotypes**

563 Field samples of Cry resistant *H. zea*, defined as surviving to late instar on a Bt corn plant
564 expressing Cry1A.105 + Cry2Ab2, were collected in 2019 and 2020 in Prince George's County
565 (MD) at the University of Maryland CMREC farm in Beltsville. Late instars were collected from
566 Cry1A.105 + Cry2Ab2 expressing sweet corn and reared in the lab on a 16:8 long day light cycle
567 at 25°C and 50% room humidity. Newly emerged adults from field collections were single pair
568 mated to produce a second generation of resistant field derived *H. zea*. Susceptible *H. zea* were
569 acquired from a population that has been maintained in the laboratory without exposure to Cry
570 toxins at Benzon Research (Cumberland County, PA). Cry tolerance in both the resistant field
571 and susceptible lab populations was measured with a diagnostic dose in a corn leaf tissue
572 incorporation assay as described in Taylor et al. (2021) to confirm resistant and susceptible
573 status. Briefly, early second instar caterpillars were fed for seven days on a laboratory diet mixed
574 with powdered lyophilized leaf tissue from Bt expressing corn and their non-Bt expressing near
575 isolines. Resistance was measured by weight gain after seven days on Bt expressing leaf diets.
576 Weight gain on the non-expressing near isoleine control diets served as a measure of non-
577 resistance associated growth.

578 The field derived progeny that grew well in the Cry expressing resistance assay (not in
579 the bottom quartile for growth) were single pair mated to a susceptible individual from the lab

580 colony. The specific susceptible individuals used in crosses were not exposed to the Cry toxin
581 resistance assay due to the significant growth suppression that would be experienced by this
582 highly susceptible population. Offspring of the single pair matings between the resistant and
583 susceptible populations were sibling mated to produce an F₂ generation. Cry toxin resistance
584 phenotypes were assessed in the F₂ progeny also using the leaf tissue incorporation assay, as
585 described in Taylor et al. (2021). Five F₂ intercross families were assessed for resistance to
586 Cry1Ab by measuring growth on diet with incorporated powdered Cry1Ab expressing leaf
587 tissue. The other half of the offspring were assayed for growth related advantages on the diets
588 with powdered leaf tissue from the non-expressing near isoline of Cry1Ab expressing corn. Five
589 different intercross families were assessed for resistance to Cry1A.105 + Cry2Ab2 by measuring
590 growth on diet with leaf tissue expressing both toxins for half of the offspring. The other half of
591 the offspring were used to assess growth related advantages on diets containing leaf tissue from
592 the non-expressing near isoline. Between 146 and 282 F₂ offspring were split across treatments
593 and phenotyped from each family, resulting in 73 to 142 F₂ offspring phenotyped per treatment
594 from each family. F₂ numbers varied due to differences in larval availability for assays. After
595 phenotyping, the larvae were grown on a non-expressing lab diet to increase in size before DNA
596 isolation. All samples were flash frozen and stored at -80°C.

597 The impact of experimental treatment and population on weight phenotypes after seven
598 days of growth in the laboratory assays was assessed using a model reduction approach between
599 nested general linear models all with a gamma distribution, as is appropriate for the continuous
600 and positive weight phenotypes (Bolker, 2008). The treatments compared were 1) Cry1Ab
601 expressing corn leaf tissue, 2) control tissue from the non-expressing near isoline of Cry1Ab
602 corn, 3) Cry1A.105 + Cry2Ab2 expressing corn leaf tissue, and 4) control tissue from the non-

603 expressing near isoline for Cry1A.105 + Cry2Ab2 corn. The populations compared were 1) the
604 resistant field derived F₀, 2) susceptible lab colony F₀, and 3) the intercross F₂ offspring. The
605 models were compared using a likelihood ratio χ^2 test with an *a priori* α of 0.01. Post hoc
606 pairwise contrasts were calculated with the R package emmeans (v. 1.8.6; Lenth et al., 2023)
607 with a bonferroni correction to p-values.

608 **DNA extraction and sequencing**

609 Individuals in the top and bottom 20% of weight phenotypes from each treatment and
610 family were selected for DNA extraction and sequencing. When individuals in the top or bottom
611 20% did not survive to preservation, they were replaced by individuals in the top or bottom 30%.
612 Genomic DNA was extracted from 833 high and low weight intercross F₂ offspring and all F₁
613 and F₀ parents with a DNeasy (Qiagen, Hilden, Germany) extraction kit using the modified
614 mouse tail protocol of Fritz et al. (2020). Larval and pupal tissue from the rear $\frac{1}{2}$ - $\frac{1}{3}$ of the
615 insect was used for extraction, while for adults, $\frac{1}{2}$ of the thorax was used. DdRAD libraries were
616 prepared for all F₂ samples as described in Fritz et al. (2016, 2018). Briefly, samples were
617 digested with the restriction enzymes EcoRI and MSPI (New England Biolabs, Ipswich, MA),
618 and unique 6-mer or 8-mer barcodes were annealed prior to pooling with 38 - 39 other samples.
619 Pools were size-selected for 450-650 bp fragments using a Pippin Prep (Sage Scientific, Beverly,
620 MA), then 12 replicated PCR reactions with 14 cycles each were used to amplify DNA and add a
621 standard Illumina TruSeq index as an identifier to each pool. Pools were sequenced at North
622 Carolina State Genomic Sciences Laboratory on an S4 flow cell of the Illumina NovaSeq 6000,
623 resulting in 173.9 - 97.5 million raw 150 bp paired-end reads per sample pool with an average of
624 128 million reads per pool. Additionally whole genome sequencing was performed for the 20
625 cross founding parents on part of an S4 flow cell of an Illumina NovaSeq 6000 at the University

626 of Maryland Baltimore Institute for Genome Science. This sequencing resulted in 30.9 - 48
627 million raw reads per sample with an average of 39.5 million raw reads.

628 **Bioinformatic analysis**

629 F_2 ddRAD sequencing reads were demultiplexed and quality controlled using the stacks
630 script process_radtags (v.2.61; Rochette et al., 2019). The reads were only retained if they had
631 exact matches to the correct barcode sequence, quality scores above 20 in all 15 bp length sliding
632 windows, and no evidence of adapter contamination allowing up to 2 bp mismatch in adapter
633 sequence. Quality controlled reads were aligned to a *H. zea* chromosome scale assembly (v. 1.0,
634 PRJNA767434; Benowitz et al., 2022) with Bowtie (v.2.2.5; Langmead & Salzberg, 2012) using
635 the “very sensitive” alignment option. Variants were called with bcftools mpileup (v. 1.9;
636 Danecek et al., 2016) and pruned to include biallelic SNPs with a minor allele frequency > 0.05 ,
637 with a quality score > 50 , present in $> 50\%$ of samples. The average sequencing coverage per
638 individual at a called ddRAD locus in the final variant set was 63 \times . The total number of ddRAD
639 sequencing markers remaining for genotype phenotype association ranged from 78,580 - 79,408
640 (Cry1Ab treatment group = 79,261, Cry1Ab control group = 79,182, Cry1A.105 + Cry2Ab2
641 treatment group = 79,408, Cry1A.105 + Cry2Ab2 control group = 78,580).

642 Whole genome sequencing reads were quality controlled with Trimmomatic (v. 0.39;
643 Bolgar et al 2014), to remove Illumina adapters, low quality regions at the beginning or end of
644 the read or where the average quality of a four base pair window fell below 30, and any reads
645 shorter than 36 bp. Trimmed reads were aligned and variants were called as described above for
646 the ddRADseq reads. In the filtered WGS data, a total of 4,716,009 high quality SNPs were
647 identified between resistant and susceptible populations, with a genome wide average sequencing
648 coverage depth of 18.6 \times (st. dev. = 2.4). For those analyses of the ddRAD sequencing data that

649 identified the direction of allele effect, SNPs were further filtered to include only those variants
650 where the allele origin (resistant or susceptible population) could be predicted with some
651 certainty. To identify SNPs where the likely origin population of the allele could be predicted,
652 only those SNPs with an allele count difference > 15 (out of a possible 20 alleles in each
653 population) between the resistant and susceptible parent populations were used. The population
654 where the allele was more common was used to identify the allele as resistance or susceptibility
655 associated. After filtering for effect direction, 6,717 - 6,749 SNPs remained (Cry1Ab treatment
656 group = 6,737, Cry1Ab control group = 6,749, Cry1A.105 + Cry2Ab2 treatment group = 6,733,
657 Cry1A.105 + Cry2Ab2 control group = 6,717).

658 **Resistant and susceptible founding populations genome wide comparison**

659 Genome-wide patterns of differentiation between the founding resistant and susceptible
660 populations were described using the variants identified by whole genome sequencing of the ten
661 field resistant and ten laboratory susceptible F₀ individuals founding the family crosses. A
662 principal components analysis was performed with Plink (v. 1.90b; Chang et al., 2015).
663 Divergence was measured by Weir and Cockerham's windowed F_{ST} across 40kb windows with a
664 10kb step using VCFtools (v. 0.1.17; Danecek et al., 2011). A genome wide zF_{ST} significance
665 threshold of 6 was used (Rubin et al., 2010). Downstream analysis of this data and all other data
666 presented here were performed in R (v.4.2.1; (R Development Core Team, 2023) with tidyverse
667 R package (v.2.0.0; Wickham et al., 2019), and visualizations were made with the R package
668 ggplot2 (v.3.4.1; Wickham, 2016)

669 **Quantitative trait mapping for Cry resistance**

670 Cry resistance genomic architecture was characterized by Bayesian sparse linear mixed
671 models (BSLMM) in gemma (v. 0.98.4; Zhou et al., 2013). For each treatment the model was run
672 five separate times, each time with a total of 5 million sampling steps with the first 500 thousand
673 discarded as burn-in. Hyperparameter estimates for each treatment were averaged across all five
674 runs. The association between SNPs across the genome and weight phenotype from the
675 resistance and control growth assays were detected with linear mixed models (LMM) also in
676 gemma (v. 0.98.4; Zhou & Stephens, 2012). Both the BSLMM and LMM account for relatedness
677 among the five replicated families for each treatment.

678 **Differential gene expression analysis**

679 In 2022, Cry1A.105 + Cry2Ab2 expressing corn ears and ears from the non-Bt
680 expressing near isoline were collected from the University of Maryland CMREC farm at
681 Beltsville. Ears that were infested with *H. zea* were identified by the loosened silk and brought to
682 the laboratory. In the lab, each corn ear was open and any 5th instar larvae present were
683 identified and removed from the ear; caterpillars at other developmental stages were not included
684 in the experiment. Immediately following removal, larvae were chilled and immobilized in a
685 70% solution of ice cold RNAlater (Invitrogen, Waltham, MA) and PBS. The head capsule on
686 each larva was removed and stored for later measurement to confirm instar. All larvae were later
687 confirmed as 5th instar by head measurements between 1.60 to 2.70 mm (Bilbo et al., 2019). The
688 midgut was cut away from the crop and intestine, and the malpighian tubules were removed.
689 Corn was cleared from midgut using forceps and a rinse of 70% RNAlater. Midguts were flash
690 frozen and stored at -80°C. The dissection process was repeated with individuals from the

691 laboratory susceptible colony, which had been reared on a standard laboratory diet not containing
692 any corn tissue or Bt toxins.

693 Midguts of 5th instars from Bt expressing corn, non-Bt corn and the susceptible
694 laboratory colony were organized into eight randomized pools per treatment with four samples in
695 each pool (n = 32 per treatment). RNA was extracted from each pool using an RNeasy® Mini
696 Kit (Qiagen, Hilden, Germany) according to the manufacturer protocol except for the initial
697 pooling of samples. Poly-A selection, library preparation, and sequencing were completed by the
698 University of Maryland Baltimore Genomics Core Facility. All RNA libraries had a RIN value
699 between 8.7 and 10, with 22/24 having RIN of 10, indicating very high quality. Libraries were
700 100 bp paired end sequenced on an Illumina NovaSeq 6000.

701 Raw reads were quality controlled with Trimmomatic (v. 0.39; Bolger et al., 2014) to
702 remove Illumina adapters, trim reads where 4 bp sliding window quality score fell below 20, and
703 drop any reads shorter than 36 bp after trimming. The paired quality controlled reads were
704 aligned to a chromosome scale *H. zea* assembly (Benowitz et al., 2022; GCA_022343045.1) with
705 HISAT2 (v. 2.2.1; Kim et al., 2019) using default parameters. Gene annotations were lifted from
706 the older reference genome Hzea_1.0 (Pearce et al., 2017; GCA_002150865.1) to the new
707 chromosome scale assembly using Liftoff (v. 1.6.1; Shumate & Salzberg, 2021). Gene
708 expression counts were generated with HTSeq-count (v. 0.13.5; Anders et al., 2015). Expression
709 patterns across all 24 pools were compared through differential expression analysis in DESeq2
710 (v. 1.38.3; Love et al., 2014). Two-way differential expression analysis was conducted between
711 resistant field individuals collected from Bt expressing corn and susceptible lab colony samples
712 to identify expression changes associated with resistance. An additional two-way differential
713 expression analysis between the field collected individuals from Bt expressing corn and non

714 expressing corn was conducted to identify Cry exposure inducible gene expression changes.
715 Statistical significance was indicated by a false discovery rate adjusted p-value of 0.01.

716 **Structural variant detection**

717 Sequencing coverage depth signals were extracted from aligned .bam files from the WGS
718 of the cross founders, the ddRAD sequencing of F₂, and two publicly available data sets. The
719 genome wide coverage depth and the average coverage depth for the trypsin cluster were
720 calculated with Qualimap (v. 2.2.1; Okonechnikov et al., 2016), while windowed coverage depth
721 calculations were from samtools depth (v. 1.10; Danecek et al., 2021) results. Calculations of
722 mean coverage of the amplified region for these analyses included all reads aligning between
723 5.22 - 5.37 Mb on Chr 9. Significant differences in coverage depth across samples were
724 determined by pairwise t-tests with a bonferroni correction to p. The presence of the structural
725 variant in 2002, 2012, and 2017 was assessed using the publicly available whole genome
726 sequencing data from Taylor et al. (2021) (PRJNA751583). The presence of the structural
727 variant in samples collected from Cry expressing and non-expressing corn was assessed using
728 sequencing data from the Pezzini et al. (2024) (PRJNA1055981).

729 The structural variant was validated with digital droplet PCR (ddPCR) for *tryp77*, one of
730 seven trypsins in the putative duplication. ATP dependent DNA helicase was used as a control
731 gene, as it is single copy in Lepidoptera in OrthoDB (Zdobnov et al., 2021). Twenty-five ng of
732 DNA per sample was mixed with HindIII and analyzed in multiplexed assay for *tryp77* and ATP
733 dependent DNA helicase at MOgene (St. Louis, MO). The genes were targeted with the primers
734 shown in (**Table S10**) and the following amplification conditions: activation at 95°C for 10
735 minutes, followed by 40 cycles of denaturing at 94°C for 30 seconds, annealing and extension at
736 58°C for 1 minute, finally the enzyme was deactivated at 98°C for 10 minutes and held at 4°C.

737 ddPCR was performed with QX200 Automated Droplet Generator and Reader and analyzed
738 using the QX Manager 1.2 Standard Edition software (Bio-Rad, Hercules CA). All samples were
739 run with a synthesized gBlock positive control and a no template negative control. Copy number
740 for samples was calculated as in Karlin-Neumann et al. (2012) with the following formula:

$$CN = \frac{\ln\left(1 - \frac{\text{target gene positive droplets}}{\text{total number of droplets}}\right)}{\ln\left(1 - \frac{\text{control gene positive droplets}}{\text{total number of droplets}}\right)} * 2$$

741
742 **Field resistant colony collection and rearing**

743 Cry resistant *H. zea* late instar caterpillars were collected from Cry1Ab expressing sweet
744 corn ('BC0805') ears grown at the Central Maryland Research and Education Center in
745 Beltsville, Maryland. Approximately 450 caterpillars were collected during each of two
746 collection dates (August 18 and September 7, 2023). Caterpillars were reared on *H. zea* diet
747 (Southland Products Inc., Arkansas, USA) until adulthood and bucket mated in a growth
748 chamber set at 25°C with 70% relative humidity and 16:8 light:dark cycle. Eggs from bucket
749 matings were placed onto diet and reared until the second instar under the same conditions.
750 Occasionally, larvae were held at 4°C once they reached the appropriate size to ensure sufficient
751 numbers at the same developmental stage for assays.

752 **Trypsin inhibition assay**

753 To determine whether trypsin activity impacts Cry toxicity in *H. zea*, we
754 compared 7-day larval weight after exposure to corn leaf tissue incorporated diet. Larvae were
755 exposed to one of 12 treatments: 1) 1X TLCK trypsin inhibitor and Cry1Ab expressing leaf
756 tissue, 2) 2X TLCK trypsin inhibitor and Cry1Ab expressing leaf tissue, 3) 5X TLCK trypsin
757 inhibitor and Cry1Ab expressing leaf tissue, 4) 10X TLCK trypsin inhibitor and Cry1Ab

758 expressing leaf tissue, 5) 1X TLCK trypsin inhibitor and non-expressing leaf tissue, 6) 2X
759 TLCK trypsin inhibitor and non-expressing leaf tissue, 7) 5X TLCK trypsin inhibitor and non-
760 expressing leaf tissue, 8) 10X TLCK trypsin inhibitor and non-expressing leaf tissue, 9) buffer
761 and Cry1Ab expressing leaf tissue, 10) buffer and non-expressing leaf tissue, 11) Cry1Ab
762 expressing leaf tissue alone, 12) non-expressing leaf tissue alone. These treatments enabled us to
763 separately determine the growth effect of Cry expressing tissue, the buffer, and the inhibitor at
764 different concentrations. Second instars from the laboratory Cry susceptible *H. zea* population
765 from Benzon research and field-collected Cry resistant *H. zea* were reared on these treatments
766 for seven days before they were individually weighed to assess growth. In each assay, 8 - 16
767 individuals were exposed to each treatment, due to availability of appropriately sized larvae.
768 Final sample sizes were ≥ 70 in each treatment, and are reported in Table S8.

769 Based upon Ma et al. (2013) and preliminary trials, we selected N- α -tosyl-L-lysine
770 chloromethyl ketone hydrochloride (TLCK, Sigma-Aldrich®, St. Louis, MO) as our trypsin
771 inhibitor. To make the inhibitor solutions, 350 mg of TLCK was dissolved in 10 mL of
772 phosphate buffer solution (0.1M, pH 5.8, bioWORLD, Dublin, OH) to make a stock solution of
773 35 mg/mL (10X). This solution was further diluted to 3.5 mg/mL (1X), 7 mg/mL (2X), and 17.5
774 mg/mL (5X) as needed. The inhibitor solutions were freshly made for each assay date. A 10 mL
775 aliquot of phosphate buffer was used for the buffer control treatment. The bioassays were
776 prepared as in Dively (2016), Taylor et al. (2021), and as described above, except, in the
777 inhibitor and buffer treatments 1.6 mL of the TLCK solution or phosphate buffer were mixed
778 into 25 mL of experimental diet, resulting in the following final TLCK concentrations: 1X: 224.5
779 μ g of TLCK per mL diet, 2X: 449 μ g of TLCK per mL diet, 5X: 1.1 mg of TLCK per mL diet,
780 10X: 2.2 mg of TLCK per mL diet.

781 First we compared the two control groups (incorporated leaf tissue only and incorporated
782 leaf tissue with buffer) using t tests with an α of 0.01 to identify any potential effects of the
783 buffer alone. Then, we tested for a synergistic effect of trypsin inhibition and Cry exposure on
784 growth in *H. zea* with a general linear model comparison approach. A gamma distribution was
785 used for the weight response variable. The fit of the models was compared with a likelihood ratio
786 chi-squared test using an α of 0.01. We tested for combined effects by comparing a full model
787 with Cry treatment and trypsin inhibition main effects and an interaction between the two, to a
788 model with only the two main effects. Bonferroni corrected post hoc contrasts were calculated
789 with the R package emmeans (v. 1.8.6; Lenth et al., 2023). We also calculated a growth ratio at
790 each TLCK dose as:

$$791 GR = \frac{\text{weight on Cry expressing leaf tissue at TLCK dose } x}{\text{weight on the non-expressing leaf tissue at TLCK dose } x}$$

792 The growth ratio measured the combined effect of TLCK and Cry toxins, and would be expected
793 to stay consistent across doses if the effects of TLCK and Cry toxins on growth suppression are
794 not linked.

795

796

797

798

799

800

801

802

803 **Acknowledgements**

804 We thank Juan Luis Jurat-Fuentes, and David Heckel for suggestions that improved our
805 manuscript. We thank Galen Dively for access to experimental plots for field collections. We
806 thank Katherine Bell, Thea Bliss, Ben Burgunder, Lasair ní Chochlain, Maria Cramer, Kyree
807 Day, Dominique Desmarattes, Shea Ill, Emma Kohanski, Ava Lamberty, Scott McCluen, Declan
808 McHugh, Oliva Moy, Hiral Patel, Daniella Anconeira Sayco, Rachel Sanford, Torsten
809 Schöneberg, Robert Starkenburg, Olivia Rosen, and Joshua Yeroshefsky for assistance with *H.*
810 *zea* collections, crosses, rearing, bioassays, and/or DNA isolation. This work was funded by the
811 US Department of Agriculture, National Institute of Food and Agriculture Biotechnology Risk
812 Assessment Grants 2019-33522-29992 and 2022-33522-37744.

813
814

815 **Figure Legends**

816 **Figure 1.** Distribution of weights for *H. zea* individuals after seven days in a laboratory leaf
817 tissue incorporation assay for Cry toxin and control treatments.

818

819 **Figure 2.** Association of genome wide markers and weight after seven days of feeding on Cry
820 toxin containing and control treatments. The additive effect (beta from LMM) is the weight in
821 mg associated with the presence of a single resistant population allele smoothed for visualization
822 by averaging over 21 SNP windows with a 5 SNP step for markers on 31 *H. zea* chromosomes.
823 The genotype-phenotype association is shown for **A.** weight after seven days of exposure to
824 Cry1Ab, **B.** weight on the non-toxin near isoline control diet for Cry1Ab, **C.** weight after seven
825 days of exposure to Cry1A.105 + Cry2Ab2, **D.** weight on the non-toxin near isoline control diet
826 for Cry1A.105 + Cry2Ab2. Chromosomes are plotted in alternating dark and light gray with each
827 point representing a 21 SNP window. Windows with at least one significantly associated SNP
828 are highlighted in color, with orange indicating an adjusted p value < 0.05 and red indicating an
829 adjusted p value < 0.01.

830

831 **Figure 3.** Genomic signals indicate that a region between 5.2 and 5.4 Mb on *H. zea* Chr 9 is
832 duplicated in field resistant individuals and associated with resistance phenotype. The absolute
833 value of the effect size (beta from the LMM) for ddRAD SNPs is plotted in **(A)**. A differential
834 expression plot for all genes on Chr 9 between resistant and susceptible populations is shown in
835 **(B)**. In **(C)** the gene annotations between 5.2 and 5.4 Mb on Chr 9 are shown above a plot of
836 relative depth of sequencing coverage for field resistant *H. zea*. Gene abbreviations are as
837 follows: Myr1 = myrosinase 1-like, Dlh = disks large homolog 4-like, Tryp = Trypsin, Npr =
838 neuropeptide receptor A35. In all panels the region between 5.2 and 5.4 Mb on Chr 9 is
839 highlighted in blue.

840

841 **Figure 4.** Resistance evolution and the gene cluster amplification on *H. zea* Chr 9. **(A)** Relative
842 sequencing depth is plotted for susceptible and resistant cross founders. In A, C, and E each
843 point represents the average sequencing depth in that 10 kb window for a single individual

844 relative to that individual's genome wide average sequencing coverage. **(B)** Coverage is
845 associated with ddPCR copy number variant analysis for *trypsin* 77 ($r^2 = 0.95$) for the resistant
846 (dark gray) and susceptible (light gray) founders of mapping families. **(C)** Relative sequencing
847 depth is plotted for individuals collected in LA in 2002 before Cry resistance evolution, 2012 as
848 resistance was evolving, and 2017 after practical resistance was first detected. **(D)** The mean
849 coverage depth of the amplified region from 5.22 - 5.37 Mb is plotted for the same individuals
850 shown in C. **(E)** Relative sequencing depth is plotted for individuals collected in 2019 in NC
851 from structured refuge, blended refuge and Cry1Ab+Cry1F expressing corn. **(F)** The mean
852 coverage depth of the amplified region is plotted for the same individuals shown in E. Coverage
853 was significantly higher for the individuals taken from Cry expressing plants compared to both
854 refuge types ($t = 2.61$, $p = 0.039$; $t = 2.67$, $p = 0.033$), suggesting selection for higher copy
855 numbers. **(G)** Mean ddRAD sequencing coverage for F_2 offspring that were the top and bottom
856 for 7 day weight in each treatment. Relative coverage was significantly higher for the F_2
857 offspring that grew largest on both toxins ($t = 3.46$, $p < 0.001$; $t = 5.21$, $p < 0.001$). On both
858 control treatments there was no relationship between coverage and growth ($t = 0.46$, $p > 0.05$; $t =$
859 -1.51 , $p > 0.05$).
860
861

862 **Figure 5.** Effect of trypsin inhibition. **(A)** Distribution of weights for laboratory susceptible and
863 field resistant *H. zea* individuals after seven days in a trypsin inhibition assay with Cry1Ab
864 containing corn leaf tissue and leaf tissue from the non-expressing near isoline. **(B)** The growth
865 ratio for each trypsin inhibitor dose, a measure of how much weight is suppressed by Cry toxins
866 and TLCK combined compared to the effects TLCK alone.

867 **References**

868 Alstad, D. N., & Andow, D. A. (1995). Managing the evolution of insect resistance to transgenic
869 plants. *Science*, 268(5219), 1894–1896. <https://doi.org/10.1126/science.268.5219.1894>

870 Amezian, D., Nauen, R., & Le Goff, G. (2021). Transcriptional regulation of xenobiotic
871 detoxification genes in insects—An overview. *Pesticide Biochemistry and Physiology*,
872 174, 104822. <https://doi.org/10.1016/j.pestbp.2021.104822>

873 Anders, S., Pyl, P. T., & Huber, W. (2015). HTSeq—A Python framework to work with high-
874 throughput sequencing data. *Bioinformatics*, 31(2), 166–169.
875 <https://doi.org/10.1093/bioinformatics/btu638>

876 Bass, C., & Field, L. M. (2011). Gene amplification and insecticide resistance. *Pest Management
877 Science*, 67(8), 886–890. <https://doi.org/10.1002/ps.2189>

878 Bass, C., Zimmer, C. T., Riveron, J. M., Wilding, C. S., Wondji, C. S., Kaussmann, M., Field, L.
879 M., Williamson, M. S., & Nauen, R. (2013). Gene amplification and microsatellite
880 polymorphism underlie a recent insect host shift. *Proceedings of the National Academy of
881 Sciences*, 110(48), 19460–19465. <https://doi.org/10.1073/pnas.1314122110>

882 Bay, R. A., Rose, N., Barrett, R., Bernatchez, L., Ghalambor, C. K., Lasky, J. R., Brem, R. B.,
883 Palumbi, S. R., & Ralph, P. (2017). Predicting responses to contemporary environmental
884 change using evolutionary response architectures. *The American Naturalist*, 189(5), 463–
885 473. <https://doi.org/10.1086/691233>

886 Benowitz, K. M., Allan, C. W., Degain, B. A., Li, X., Fabrick, J. A., Tabashnik, B. E., Carrière,
887 Y., & Matzkin, L. M. (2022). Novel genetic basis of resistance to Bt toxin Cry1Ac in
888 *Helicoverpa zea*. *Genetics*, 221(1), iyac037. <https://doi.org/10.1093/genetics/iyac037>

889 Bergland, A. O., Behrman, E. L., O'Brien, K. R., Schmidt, P. S., & Petrov, D. A. (2014).
890 Genomic evidence of rapid and stable adaptive oscillations over seasonal time scales in
891 *Drosophila*. *PLOS Genetics*, 10(11), e1004775.
892 <https://doi.org/10.1371/journal.pgen.1004775>

893 Bi, K., Linderoth, T., Singhal, S., Vanderpool, D., Patton, J. L., Nielsen, R., Moritz, C., & Good,
894 J. M. (2019). Temporal genomic contrasts reveal rapid evolutionary responses in an
895 alpine mammal during recent climate change. *PLOS Genetics*, 15(5), e1008119.
896 <https://doi.org/10.1371/journal.pgen.1008119>

897 Bilbo, T. R., Reay-Jones, F. P. F., Reisig, D. D., Greene, J. K., & Turnbull, M. W. (2019).
898 Development, survival, and feeding behavior of *Helicoverpa zea* (Lepidoptera:
899 Noctuidae) relative to Bt protein concentrations in corn ear tissues. *PLoS ONE*, 14(8),
900 e0221343. <https://doi.org/10.1371/journal.pone.0221343>

901 Bolger, A. M., Lohse, M., & Usadel, B. (2014). Trimmomatic: A flexible trimmer for Illumina
902 sequence data. *Bioinformatics*, 30(15), 2114–2120.
903 <https://doi.org/10.1093/bioinformatics/btu170>

904 Bolker, B. M. (2008). Ecological models and data in R. In *Ecological Models and Data in R*.

905 Princeton University Press. <https://doi.org/10.1515/9781400840908>

906 Brévault, T., Heuberger, S., Zhang, M., Ellers-Kirk, C., Ni, X., Masson, L., Li, X., Tabashnik, B.
907 E., & Carrière, Y. (2013). Potential shortfall of pyramided transgenic cotton for insect
908 resistance management. *Proceedings of the National Academy of Sciences*, 110(15),
909 5806–5811. <https://doi.org/10.1073/pnas.1216719110>

910 Brevik, K., Schoville, S. D., Mota-Sanchez, D., & Chen, Y. H. (2018). Pesticide durability and
911 the evolution of resistance: A novel application of survival analysis. *Pest Management
912 Science*, 74(8), 1953–1963. <https://doi.org/10.1002/ps.4899>

913 Campbell-Staton, S. C., Cheviron, Z. A., Rochette, N., Catchen, J., Losos, J. B., & Edwards, S.
914 V. (2017). Winter storms drive rapid phenotypic, regulatory, and genomic shifts in the
915 green anole lizard. *Science*, 357(6350), 495–498.
916 <https://doi.org/10.1126/science.aam5512>

917 Cattaneo, M. G., Yafuso, C., Schmidt, C., Huang, C., Rahman, M., Olson, C., Ellers-Kirk, C.,
918 Orr, B. J., Marsh, S. E., Antilla, L., Dutilleul, P., & Carrière, Y. (2006). Farm-scale
919 evaluation of the impacts of transgenic cotton on biodiversity, pesticide use, and yield.
920 *Proceedings of the National Academy of Sciences*, 103(20), 7571–7576.
921 <https://doi.org/10.1073/pnas.0508312103>

922 Cattel, J., Haberkorn, C., Laporte, F., Gaude, T., Cumér, T., Renaud, J., Sutherland, I. W., Hertz,
923 J. C., Bonneville, J.-M., Arnaud, V., Fustec, B., Boyer, S., Marcombe, S., & David, J.-P.
924 (2021). A genomic amplification affecting a carboxylesterase gene cluster confers
925 organophosphate resistance in the mosquito *Aedes aegypti*: From genomic
926 characterization to high-throughput field detection. *Evolutionary Applications*, 14(4),
927 1009–1022. <https://doi.org/10.1111/eva.13177>

928 Chang, C. C., Chow, C. C., Tellier, L. C., Vattikuti, S., Purcell, S. M., & Lee, J. J. (2015).
929 Second-generation PLINK: Rising to the challenge of larger and richer datasets.
930 *GigaScience*, 4(1). <https://doi.org/10.1186/s13742-015-0047-8>

931 Chaturvedi, A., Zhou, J., Raeymaekers, J. A. M., Czypionka, T., Orsini, L., Jackson, C. E.,
932 Spanier, K. I., Shaw, J. R., Colbourne, J. K., & De Meester, L. (2021). Extensive standing
933 genetic variation from a small number of founders enables rapid adaptation in *Daphnia*.
934 *Nature Communications*, 12(1), 4306. <https://doi.org/10.1038/s41467-021-24581-z>

935 Chen, Y., & Schoville, S. (2018). Editorial overview: Ecology: Ecological adaptation in
936 agroecosystems: novel opportunities to integrate evolutionary biology and agricultural
937 entomology. *Current Opinion in Insect Science*, 26, iv–viii.
938 <https://doi.org/10.1016/j.cois.2018.03.003>

939 Clark, B. W., Phillips, T. A., & Coats, J. R. (2005). Environmental fate and effects of *Bacillus
940 thuringiensis* (Bt) proteins from transgenic crops: A review. *Journal of Agricultural and
941 Food Chemistry*, 53(12), 4643–4653. <https://doi.org/10.1021/jf040442k>

942 Correy, G. J., Zaidman, D., Harmelin, A., Carvalho, S., Mabbitt, P. D., Calaora, V., James, P. J.,
943 Kotze, A. C., Jackson, C. J., & London, N. (2019). Overcoming insecticide resistance

944 through computational inhibitor design. *Proceedings of the National Academy of*
945 *Sciences*, 116(42), 21012–21021. <https://doi.org/10.1073/pnas.1909130116>

946 Danecek, P., Auton, A., Abecasis, G., Albers, C. A., Banks, E., DePristo, M. A., Handsaker, R.
947 E., Lunter, G., Marth, G. T., Sherry, S. T., McVean, G., Durbin, R., & 1000 Genomes
948 Project Analysis Group. (2011). The variant call format and VCFtools. *Bioinformatics*,
949 27(15), 2156–2158. <https://doi.org/10.1093/bioinformatics/btr330>

950 Danecek, P., Schiffels, S., & Durbin, R. (2016). *Multiallelic calling model in bcftools (-m)*,
951 samtools.github.io/bcftools/call-m.pdf [Computer software].

952 Davey, J. W., Cezard, T., Fuentes-Utrilla, P., Eland, C., Gharbi, K., & Blaxter, M. L. (2013).
953 Special features of RAD sequencing data: Implications for genotyping. *Molecular*
954 *Ecology*, 22(11), 3151–3164. <https://doi.org/10.1111/mec.12084>

955 Dively, G. P., Huang, F., Oyediran, I., Burd, T., & Morsello, S. (2020). Evaluation of gene flow
956 in structured and seed blend refuge systems of non-Bt and Bt corn. *Journal of Pest*
957 *Science*, 93(1), 439–447. <https://doi.org/10.1007/s10340-019-01126-4>

958 Dively, G. P., Venugopal, P. D., Bean, D., Whalen, J., Holmstrom, K., Kuhar, T. P., Doughty, H.
959 B., Patton, T., Cissel, W., & Hutchison, W. D. (2018). Regional pest suppression
960 associated with widespread Bt maize adoption benefits vegetable growers. *Proceedings*
961 *of the National Academy of Sciences*, 115(13), 3320–3325.
962 <https://doi.org/10.1073/pnas.1720692115>

963 Dively, G. P., Venugopal, P. D., & Finkenbinder, C. (2016). Field-evolved resistance in corn
964 earworm to Cry proteins expressed by transgenic sweet corn. *PLOS ONE*, 11(12),
965 e0169115. <https://doi.org/10.1371/journal.pone.0169115>

966 Ergon, Å., Skøt, L., Sæther, V. E., & Rognli, O. A. (2019). Allele frequency changes provide
967 evidence for selection and identification of candidate loci for survival in red clover
968 (*Trifolium pratense L.*). *Frontiers in Plant Science*, 10.
969 <https://doi.org/10.3389/fpls.2019.00718>

970 Falconer, D. S. (1996). *Introduction to quantitative genetics* (4th ed). Prentice Hall.

971 Fritz, M. L. (2022). Utility and challenges of using whole-genome resequencing to detect
972 emerging insect and mite resistance in agroecosystems. *Evolutionary Applications*,
973 15(10), 1505–1520. <https://doi.org/10.1111/eva.13484>

974 Fritz, M. L., DeYonke, A. M., Papanicolaou, A., Micinski, S., Westbrook, J., & Gould, F.
975 (2018). Contemporary evolution of a Lepidopteran species, *Heliothis virescens*, in
976 response to modern agricultural practices. *Molecular Ecology*, 27(1), 167–181.
977 <https://doi.org/10.1111/mec.14430>

978 Fritz, M. L., Paa, S., Baltzegar, J., & Gould, F. (2016). Application of a dense genetic map for
979 assessment of genomic responses to selection and inbreeding in *Heliothis virescens*.
980 *Insect Molecular Biology*, 25(4), 385–400. <https://doi.org/10.1111/imb.12234>

981 Frutos, R., Rang, C., & Royer, M. (1999). Managing insect resistance to plants producing

982 *Bacillus thuringiensis* toxins. *Critical Reviews in Biotechnology*, 19(3), 227–276.
983 <https://doi.org/10.1080/0738-859991229251>

984 Gassmann, A. J., & Reisig, D. D. (2023). Management of insect pests with Bt crops in the United
985 States. *Annual Review of Entomology*, 68(1). <https://doi.org/10.1146/annurev-ento-120220-105502>

987 Gong, L., Kang, S., Zhou, J., Sun, D., Guo, L., Qin, J., Zhu, L., Bai, Y., Ye, F., Akami, M., Wu,
988 Q., Wang, S., Xu, B., Yang, Z., Bravo, A., Soberón, M., Guo, Z., Wen, L., & Zhang, Y.
989 (2020). Reduced expression of a novel midgut trypsin gene involved in protoxin
990 activation correlates with Cry1Ac resistance in a laboratory-selected strain of *Plutella*
991 *xylostella* (L.). *Toxins*, 12(2), Article 2. <https://doi.org/10.3390/toxins12020076>

992 González-Cabrera, J., García, M., Hernández-Crespo, P., Farinós, G. P., Ortego, F., & Castañera,
993 P. (2013). Resistance to Bt maize in *Mythimna unipuncta* (Lepidoptera: Noctuidae) is
994 mediated by alteration in Cry1Ab protein activation. *Insect Biochemistry and Molecular
995 Biology*, 43(8), 635–643. <https://doi.org/10.1016/j.ibmb.2013.04.001>

996 Gould, F. (1998). Sustainability of transgenic insecticidal cultivars: Integrating pest genetics and
997 ecology. *Annual Review of Entomology*, 43(1), 701–726.
998 <https://doi.org/10.1146/annurev.ento.43.1.701>

999 Gould, F., Brown, Z. S., & Kuzma, J. (2018). Wicked evolution: Can we address the
1000 sociobiological dilemma of pesticide resistance? *Science*, 360(6390), 728–732.
1001 <https://doi.org/10.1126/science.aar3780>

1002 Guo, Z., Kang, S., Wu, Q., Wang, S., Crickmore, N., Zhou, X., Bravo, A., Soberón, M., &
1003 Zhang, Y. (2021). The regulation landscape of MAPK signaling cascade for thwarting
1004 *Bacillus thuringiensis* infection in an insect host. *PLOS Pathogens*, 17(9), e1009917.
1005 <https://doi.org/10.1371/journal.ppat.1009917>

1006 Heckel, D. G. (2020). How do toxins from *Bacillus thuringiensis* kill insects? An evolutionary
1007 perspective. *Archives of Insect Biochemistry and Physiology*, 104(2), e21673.
1008 <https://doi.org/10.1002/arch.21673>

1009 Heckel, D. G. (2022). Perspectives on gene copy number variation and pesticide resistance. *Pest
1010 Management Science*, 78(1), 12–18. <https://doi.org/10.1002/ps.6631>

1011 Herrero, S., Gechev, T., Bakker, P. L., Moar, W. J., & de Maagd, R. A. (2005). *Bacillus
1012 thuringiensis* Cry1Ca-resistant *Spodoptera exigua* lacks expression of one of four
1013 Aminopeptidase N genes. *BMC Genomics*, 6(1), 96. <https://doi.org/10.1186/1471-2164-6-96>

1015 Ho, S. S., Urban, A. E., & Mills, R. E. (2020). Structural variation in the sequencing era. *Nature
1016 Reviews Genetics*, 21(3), Article 3. <https://doi.org/10.1038/s41576-019-0180-9>

1017 Horner, T. A., Dively, G. P., & Herbert, D. A. (2003). Development, survival and fitness
1018 performance of *Helicoverpa zea* (Lepidoptera: Noctuidae) in MON810 Bt field corn.
1019 *Journal of Economic Entomology*, 96(3), 914–924. <https://doi.org/10.1093/jee/96.3.914>

1020 Hutchison, W. D., Burkness, E. C., Mitchell, P. D., Moon, R. D., Leslie, T. W., Fleischer, S. J.,
1021 Abrahamson, M., Hamilton, K. L., Steffey, K. L., Gray, M. E., Hellmich, R. L., Kaster,
1022 L. V., Hunt, T. E., Wright, R. J., Pecinovsky, K., Rabaey, T. L., Flood, B. R., & Raun, E.
1023 S. (2010). Areawide suppression of European corn borer with Bt maize reaps savings to
1024 non-Bt maize growers. *Science*, 330(6001), 222–225.
1025 <https://doi.org/10.1126/science.1190242>

1026 Jurat-Fuentes, J. L., Heckel, D. G., & Ferré, J. (2021). Mechanisms of resistance to insecticidal
1027 proteins from *Bacillus thuringiensis*. *Annual Review of Entomology*, 66(1), 121–140.
1028 <https://doi.org/10.1146/annurev-ento-052620-073348>

1029 Karlin-Neumann, G., Montesclaros, L., Heredia, N., Hodges, S., Regan, J., Troup, C.,
1030 Mukhopadhyay, D., & Litterst, C. (2012). *Probing copy number variations using Bio-*
1031 *Rad's QX100™ Droplet Digital™ PCR system*.

1032 Kathage, J., & Qaim, M. (2012). Economic impacts and impact dynamics of Bt (*Bacillus*
1033 *thuringiensis*) cotton in India. *Proceedings of the National Academy of Sciences*, 109(29),
1034 11652–11656. <https://doi.org/10.1073/pnas.1203647109>

1035 Kim, D., Paggi, J. M., Park, C., Bennett, C., & Salzberg, S. L. (2019). Graph-based genome
1036 alignment and genotyping with HISAT2 and HISAT-genotype. *Nature Biotechnology*,
1037 37(8), Article 8. <https://doi.org/10.1038/s41587-019-0201-4>

1038 Kondrashov, F. A. (2012). Gene duplication as a mechanism of genomic adaptation to a
1039 changing environment. *Proceedings. Biological Sciences*, 279(1749), 5048–5057.
1040 <https://doi.org/10.1098/rspb.2012.1108>

1041 Langmead, B., & Salzberg, S. L. (2012). Fast gapped-read alignment with Bowtie 2. *Nature*
1042 *Methods*, 9(4), 357–359. <https://doi.org/10.1038/nmeth.1923>

1043 Lawrie, R. D., Mitchell Iii, R. D., Deguenon, J. M., Ponnusamy, L., Reisig, D., Pozo-Valdivia,
1044 A. D., Kurtz, R. W., & Roe, R. M. (2020). Multiple known mechanisms and a possible
1045 role of an enhanced immune system in Bt-resistance in a field population of the
1046 Bollworm, *Helicoverpa zea* : Differences in gene expression with RNAseq. *International*
1047 *Journal of Molecular Sciences*, 21(18), E6528. <https://doi.org/10.3390/ijms21186528>

1048 Lenth, R. V., Bolker, B., Buerkner, P., Giné-Vázquez, I., Herve, M., Jung, M., Love, J., Miguez,
1049 F., Riebl, H., & Singmann, H. (2023). *emmeans: Estimated Marginal Means, aka Least-*
1050 *Squares Means* (1.8.7) [Computer software]. [https://cran.r-](https://cran.r-project.org/web/packages/emmeans/index.html)
1051 [project.org/web/packages/emmeans/index.html](https://cran.r-project.org/web/packages/emmeans/index.html)

1052 Liu, C., Xiao, Y., Li, X., Oppert, B., Tabashnik, B. E., & Wu, K. (2014). Cis-mediated down-
1053 regulation of a trypsin gene associated with Bt resistance in cotton bollworm. *Scientific*
1054 *Reports*, 4(1), Article 1. <https://doi.org/10.1038/srep07219>

1055 Liu, L., Li, Z., Luo, X., Zhang, X., Chou, S.-H., Wang, J., & He, J. (2021). Which is stronger? A
1056 continuing battle between Cry toxins and insects. *Frontiers in Microbiology*, 12.
1057 <https://www.frontiersin.org/article/10.3389/fmicb.2021.665101>

1058 Love, M. I., Huber, W., & Anders, S. (2014). Moderated estimation of fold change and
1059 dispersion for RNA-seq data with DESeq2. *Genome Biology*, 15(12), 550.
1060 <https://doi.org/10.1186/s13059-014-0550-8>

1061 Luttrell, R. G., Wan, L., & Knighten, K. (1999). Variation in susceptibility of Noctuid
1062 (Lepidoptera) larvae attacking cotton and soybean to purified endotoxin proteins and
1063 commercial formulations of *Bacillus thuringiensis*. *Journal of Economic Entomology*,
1064 92(1), 21–32. <https://doi.org/10.1093/jee/92.1.21>

1065 Lynch, M., & Walsh, B. (1998). *Genetics and analysis of quantitative traits*. Sinauer.

1066 Ma, X., Shao, E., Chen, W., Cotto-Rivera, R. O., Yang, X., Kain, W., Fei, Z., & Wang, P.
1067 (2022). Bt Cry1Ac resistance in *Trichoplusia ni* is conferred by multi-gene mutations.
1068 *Insect Biochemistry and Molecular Biology*, 140, 103678.
1069 <https://doi.org/10.1016/j.ibmb.2021.103678>

1070 Ma, Y., Zhang, Y., Chen, R.-R., Ren, X.-L., Wan, P.-J., Mu, L.-L., & Li, G.-Q. (2013).
1071 Combined effects of three crystalline toxins from *Bacillus thuringiensis* with seven
1072 proteinase inhibitors on beet armyworm, *Spodoptera exigua* Hübner (Lepidoptera:
1073 Noctuidae). *Pesticide Biochemistry and Physiology*, 105(3), 169–176.
1074 <https://doi.org/10.1016/j.pestbp.2013.01.007>

1075 Mahmoud, M., Gobet, N., Cruz-Dávalos, D. I., Mounier, N., Dessimoz, C., & Sedlazeck, F. J.
1076 (2019). Structural variant calling: The long and the short of it. *Genome Biology*, 20(1),
1077 246. <https://doi.org/10.1186/s13059-019-1828-7>

1078 McGaughey, W., Gould, F., & Gelernter, W. (1998). Bt resistance management. *Nature
1079 Biotechnology*, 16, 144–146. <https://doi.org/10.1038/nbt0298-144>

1080 McKenzie, J. A., & Batterham, P. (1994). The genetic, molecular and phenotypic consequences
1081 of selection for insecticide resistance. *Trends in Ecology & Evolution*, 9(5), 166–169.
1082 [https://doi.org/10.1016/0169-5347\(94\)90079-5](https://doi.org/10.1016/0169-5347(94)90079-5)

1083 Mikheyev, A. S., Tin, M. M. Y., Arora, J., & Seeley, T. D. (2015). Museum samples reveal rapid
1084 evolution by wild honey bees exposed to a novel parasite. *Nature Communications*, 6(1),
1085 7991. <https://doi.org/10.1038/ncomms8991>

1086 Mota-Sánchez, D., & Wise, J. C. (2022). *The arthropod pesticide resistance database*.
1087 www.pesticideresistance.org/search.php

1088 Mouches, C., Pauplin, Y., Agarwal, M., Lemieux, L., Herzog, M., Abadon, M., Beyssat-
1089 Arnaouty, V., Hyrien, O., De Saint Vincent, B. R., & Georghiou, G. P. (1990).
1090 Characterization of amplification core and esterase B1 gene responsible for insecticide
1091 resistance in *Culex*. *Proceedings of the National Academy of Sciences*, 87(7), 2574–2578.
1092 <https://doi.org/10.1073/pnas.87.7.2574>

1093 Muhlia-Almazán, A., Sánchez-Paz, A., & García-Carreño, F. L. (2008). Invertebrate trypsin: A
1094 review. *Journal of Comparative Physiology B*, 178(6), 655–672.
1095 <https://doi.org/10.1007/s00360-008-0263-y>

1096 Nauen, R., Bass, C., Feyereisen, R., & Vontas, J. (2022). The role of cytochrome P450s in insect
1097 toxicology and resistance. *Annual Review of Entomology*, 67(1), 105–124.
1098 <https://doi.org/10.1146/annurev-ento-070621-061328>

1099 Palumbi, S. R. (2001). Humans as the world's greatest evolutionary force. *Science*, 293(5536),
1100 1786–1790.

1101 Pearce, S. L., Clarke, D. F., East, P. D., Elfekih, S., Gordon, K. H. J., Jermini, L. S.,
1102 McGaughan, A., Oakeshott, J. G., Papanikolaou, A., Perera, O. P., Rane, R. V.,
1103 Richards, S., Tay, W. T., Walsh, T. K., Anderson, A., Anderson, C. J., Asgari, S., Board,
1104 P. G., Bretschneider, A., ... Wu, Y. D. (2017). Genomic innovations, transcriptional
1105 plasticity and gene loss underlying the evolution and divergence of two highly
1106 polyphagous and invasive *Helicoverpa* pest species. *BMC Biology*, 15(1), 63.
1107 <https://doi.org/10.1186/s12915-017-0402-6>

1108 Perry, E. D., Ciliberto, F., Hennessy, D. A., & Moschini, G. (2016). Genetically engineered
1109 crops and pesticide use in U.S. maize and soybeans. *Science Advances*, 2(8), e1600850.
1110 <https://doi.org/10.1126/sciadv.1600850>

1111 Puinean, A. M., Foster, S. P., Oliphant, L., Denholm, I., Field, L. M., Millar, N. S., Williamson,
1112 M. S., & Bass, C. (2010). Amplification of a cytochrome P450 gene is associated with
1113 resistance to neonicotinoid insecticides in the aphid *Myzus persicae*. *PLOS Genetics*,
1114 6(6), e1000999. <https://doi.org/10.1371/journal.pgen.1000999>

1115 R Development Core Team. (2023). *R: A language and environment for statistical computing*. R
1116 Foundation for Statistical Computing. <http://www.R-project.org>.

1117 Reisig, D. D. (2017). Factors associated with willingness to plant non-Bt maize refuge and
1118 suggestions for increasing refuge compliance. *Journal of Integrated Pest Management*,
1119 8(1), 9. <https://doi.org/10.1093/jipm/pmx002>

1120 Reisig, D. D., Huseth, A. S., Bacheler, J. S., Aghaee, M.-A., Braswell, L., Burrack, H. J.,
1121 Flanders, K., Greene, J. K., Herbert, D. A., Jacobson, A., Paula-Moraes, S. V., Roberts,
1122 P., & Taylor, S. V. (2018). Long-term empirical and observational evidence of practical
1123 *Helicoverpa zea* resistance to cotton with pyramided Bt toxins. *Journal of Economic
1124 Entomology*, 111(4), 1824–1833. <https://doi.org/10.1093/jee/toy106>

1125 Reisig, D. D., & Kurtz, R. (2018). Bt resistance implications for *Helicoverpa zea* (Lepidoptera:
1126 Noctuidae) insecticide resistance management in the United States. *Environmental
1127 Entomology*, 47(6), 1357–1364. <https://doi.org/10.1093/ee/nvy142>

1128 Roberts Kingman, G. A., Vyas, D. N., Jones, F. C., Brady, S. D., Chen, H. I., Reid, K.,
1129 Milhaven, M., Bertino, T. S., Aguirre, W. E., Heins, D. C., von Hippel, F. A., Park, P. J.,
1130 Kirch, M., Absher, D. M., Myers, R. M., Di Palma, F., Bell, M. A., Kingsley, D. M., &
1131 Veeramah, K. R. (2021). Predicting future from past: The genomic basis of recurrent and
1132 rapid stickleback evolution. *Science Advances*, 7(25), eabg5285.
1133 <https://doi.org/10.1126/sciadv.abg5285>

1134 Rochette, N. C., Rivera-Colón, A. G., & Catchen, J. M. (2019). Stacks 2: Analytical methods for

1135 paired-end sequencing improve RADseq-based population genomics. *Molecular Ecology*,
1136 28(21), 4737–4754. <https://doi.org/10.1111/mec.15253>

1137 Rubin, C. J., Zody, M. C., Eriksson, J., Meadows, J. R. S., Sherwood, E., Webster, M. T., Jiang,
1138 L., Ingman, M., Sharpe, T., Ka, S., Hallböök, F., Besnier, F., Carlberg, Ö., Bed'hom, B.,
1139 Tixier-Boichard, M., Jensen, P., Siegel, P., Lindblad-Toh, K., & Andersson, L. (2010).
1140 Whole-genome resequencing reveals loci under selection during chicken domestication.
1141 *Nature*, 464(7288), Article 7288. <https://doi.org/10.1038/nature08832>

1142 Rudman, S. M., Greenblum, S. I., Rajpurohit, S., Betancourt, N. J., Hanna, J., Tilk, S.,
1143 Yokoyama, T., Petrov, D. A., & Schmidt, P. (2022). Direct observation of adaptive
1144 tracking on ecological time scales in *Drosophila*. *Science*, 375(6586), eabj7484.
1145 <https://doi.org/10.1126/science.abj7484>

1146 Schiebelhut, L. M., Puritz, J. B., & Dawson, M. N. (2018). Decimation by sea star wasting
1147 disease and rapid genetic change in a keystone species, *Pisaster ochraceus*. *Proceedings
1148 of the National Academy of Sciences*, 115(27), 7069–7074.
1149 <https://doi.org/10.1073/pnas.1800285115>

1150 Schmidt, J. M., Good, R. T., Appleton, B., Sherrard, J., Raymant, G. C., Bogwitz, M. R., Martin,
1151 J., Daborn, P. J., Goddard, M. E., Batterham, P., & Robin, C. (2010). Copy number
1152 variation and transposable elements feature in recent, ongoing adaptation at the Cyp6g1
1153 locus. *PLOS Genetics*, 6(6), e1000998. <https://doi.org/10.1371/journal.pgen.1000998>

1154 Stahlke, A. R., Epstein, B., Barbosa, S., Margres, M. J., Patton, A. H., Hendricks, S. A., Veillet,
1155 A., Fraik, A. K., Schönfeld, B., McCallum, H. I., Hamede, R., Jones, M. E., Storfer, A.,
1156 & Hohenlohe, P. A. (2021). Contemporary and historical selection in Tasmanian devils
1157 (*Sarcophilus harrisii*) support novel, polygenic response to transmissible cancer.
1158 *Proceedings of the Royal Society B: Biological Sciences*, 288(1951), 20210577.
1159 <https://doi.org/10.1098/rspb.2021.0577>

1160 Storz, J. F., & Wheat, C. W. (2010). Integrating evolutionary and functional approaches to infer
1161 adaptation at specific loci. *Evolution*, 64(9), 2489–2509. [https://doi.org/10.1111/j.1558-5646.2010.01044.x](https://doi.org/10.1111/j.1558-
1162 5646.2010.01044.x)

1163 Sun, D., Zhu, L., Guo, L., Wang, S., Wu, Q., Crickmore, N., Zhou, X., Bravo, A., Soberón, M.,
1164 Guo, Z., & Zhang, Y. (2022). A versatile contribution of both aminopeptidases N and
1165 ABC transporters to Bt Cry1Ac toxicity in the diamondback moth. *BMC Biology*, 20(1),
1166 33. <https://doi.org/10.1186/s12915-022-01226-1>

1167 Székács, A., Lauber, É., Juracsek, J., & Darvas, B. (2010). Cry1Ab toxin production of MON
1168 810 transgenic maize. *Environmental Toxicology and Chemistry*, 29(1), 182–190.
1169 <https://doi.org/10.1002/etc.5>

1170 Tabashnik, B. E., & Carrière, Y. (2017). Surge in insect resistance to transgenic crops and
1171 prospects for sustainability. *Nature Biotechnology*, 35(10), 926–935.
1172 <https://doi.org/10.1038/nbt.3974>

1173 Taylor, K. L., Hamby, K. A., DeYonke, A. M., Gould, F., & Fritz, M. L. (2021). Genome

1174 evolution in an agricultural pest following adoption of transgenic crops. *Proceedings of*
1175 *the National Academy of Sciences*, 118(52). <https://doi.org/10.1073/pnas.2020853118>

1176 US-EPA. (2018). *White Paper on Resistance in Lepidopteran Pests of Bacillus thuringiensis (Bt)*
1177 *Plant-incorporated Protectants in the United States*.

1178 Wickham, H. (2016). *ggplot2: Elegant Graphics for Data Analysis*. Springer.

1179 Wickham, H., Averick, M., Bryan, J., Chang, W., McGowan, L. D., François, R., Grolemund,
1180 G., Hayes, A., Henry, L., Hester, J., Kuhn, M., Pedersen, T. L., Miller, E., Bache, S. M.,
1181 Müller, K., Ooms, J., Robinson, D., Seidel, D. P., Spinu, V., ... Yutani, H. (2019).
1182 Welcome to the Tidyverse. *Journal of Open Source Software*, 4(43), 1686.
1183 <https://doi.org/10.21105/joss.01686>

1184 Wilding, C. S. (2018). Regulating resistance: CncC:Maf, antioxidant response elements and the
1185 overexpression of detoxification genes in insecticide resistance. *Current Opinion in*
1186 *Insect Science*, 27, 89–96. <https://doi.org/10.1016/j.cois.2018.04.006>

1187 Yang, F., González, J. C. S., Williams, J., Cook, D. C., Gilreath, R. T., & Kerns, D. L. (2019).
1188 Occurrence and ear damage of *Helicoverpa zea* on transgenic *Bacillus thuringiensis*
1189 maize in the field in Texas, U.S. and its susceptibility to Vip3A protein. *Toxins*, 11(2),
1190 Article 2. <https://doi.org/10.3390/toxins11020102>

1191 Yang, F., Kerns, D., & Huang, F. (2015). Refuge-in-the-bag strategy for managing insect
1192 resistance to Bt maize. *Outlooks on Pest Management*, 26(5), 226–228.
1193 https://doi.org/10.1564/v26_oct_10

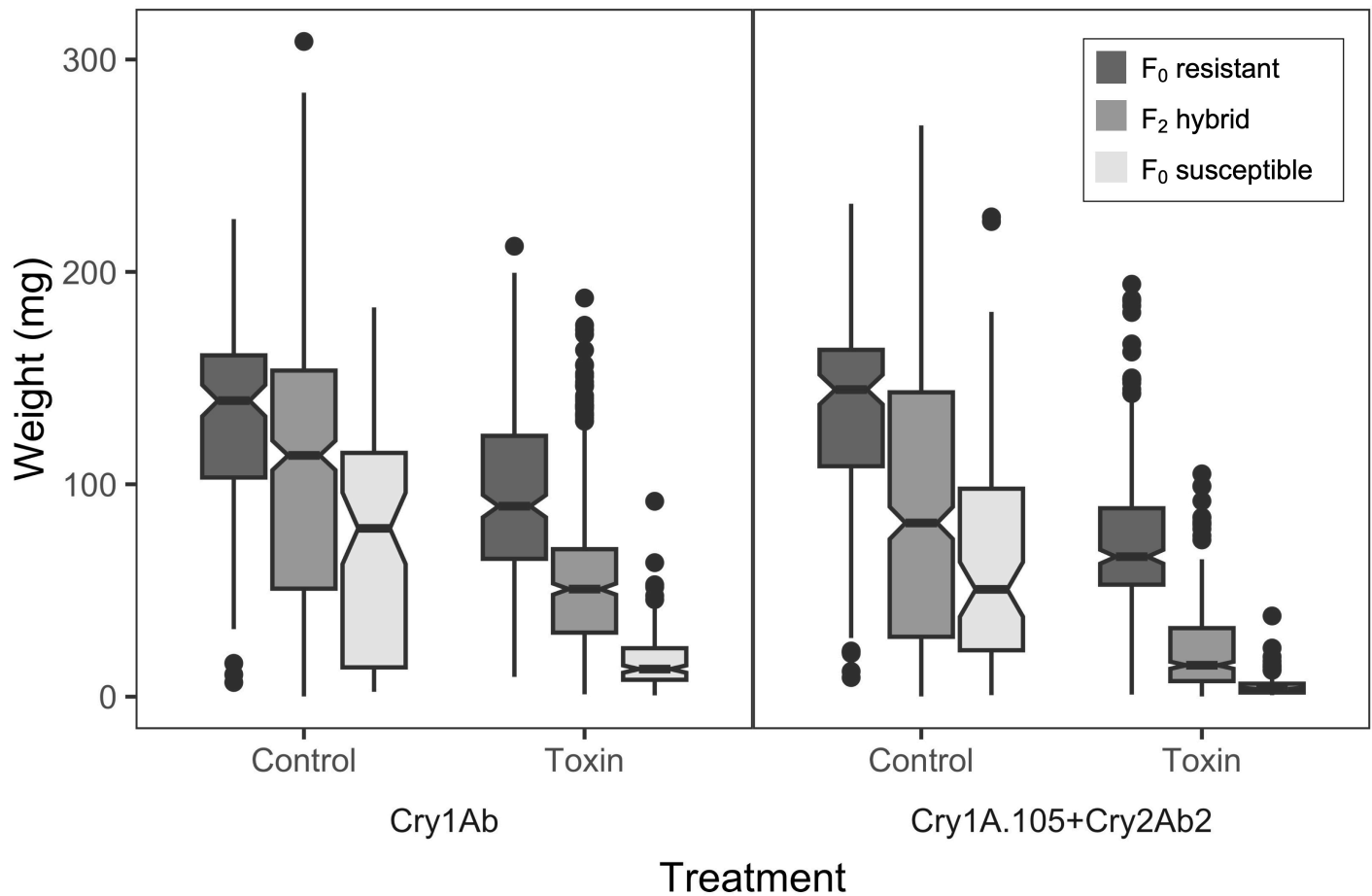
1194 Yang, F., Kerns, D. L., Little, N., Brown, S. A., Stewart, S. D., Catchot, A. L., Cook, D. R.,
1195 Gore, J., Crow, W. D., Lorenz, G. M., Towles, T., & Tabashnik, B. E. (2022). Practical
1196 resistance to Cry toxins and efficacy of Vip3Aa in Bt cotton against *Helicoverpa zea*.
1197 *Pest Management Science*, 78(12), 5234–5242. <https://doi.org/10.1002/ps.7142>

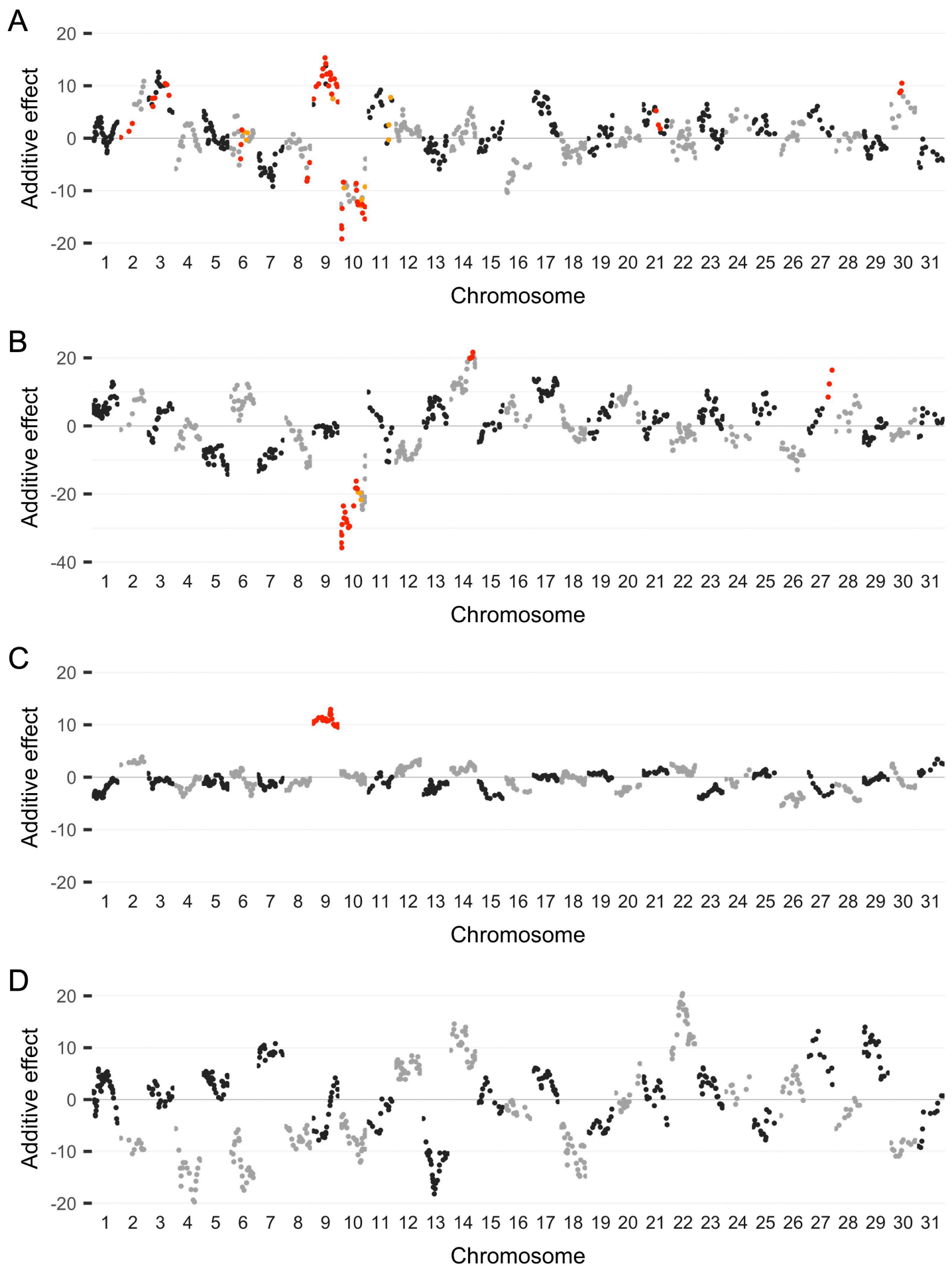
1198 Zdobnov, E. M., Kuznetsov, D., Tegenfeldt, F., Manni, M., Berkeley, M., & Kriventseva, E. V.
1199 (2021). OrthoDB in 2020: Evolutionary and functional annotations of orthologs. *Nucleic*
1200 *Acids Research*, 49(D1), D389–D393. <https://doi.org/10.1093/nar/gkaa1009>

1201 Zhang, M., Wei, J., Ni, X., Zhang, J., Jurat-Fuentes, J. L., Fabrick, J. A., Carrière, Y., Tabashnik,
1202 B. E., & Li, X. (2019). Decreased Cry1Ac activation by midgut proteases associated with
1203 Cry1Ac resistance in *Helicoverpa zea*. *Pest Management Science*, 75(4), 1099–1106.
1204 <https://doi.org/10.1002/ps.5224>

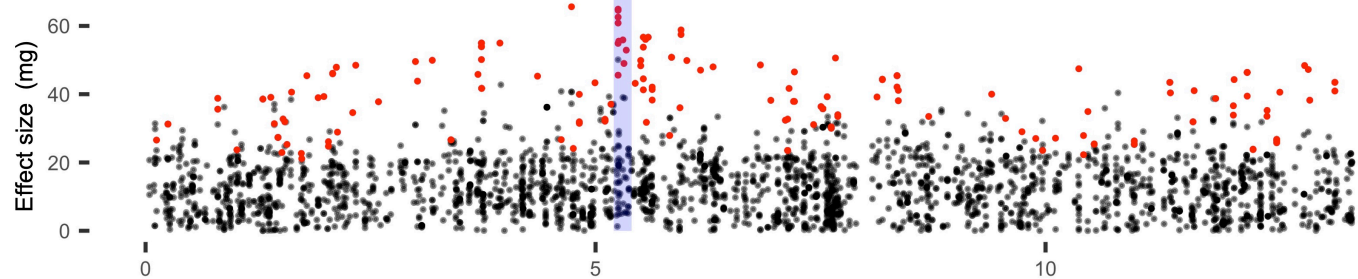
1205 Zhou, X., Carbonetto, P., & Stephens, M. (2013). Polygenic modeling with Bayesian sparse
1206 linear mixed models. *PLOS Genetics*, 9(2), e1003264.
1207 <https://doi.org/10.1371/journal.pgen.1003264>

1208 Zhou, X., & Stephens, M. (2012). Genome-wide efficient mixed-model analysis for association
1209 studies. *Nature Genetics*, 44(7), 821–824. <https://doi.org/10.1038/ng.2310>

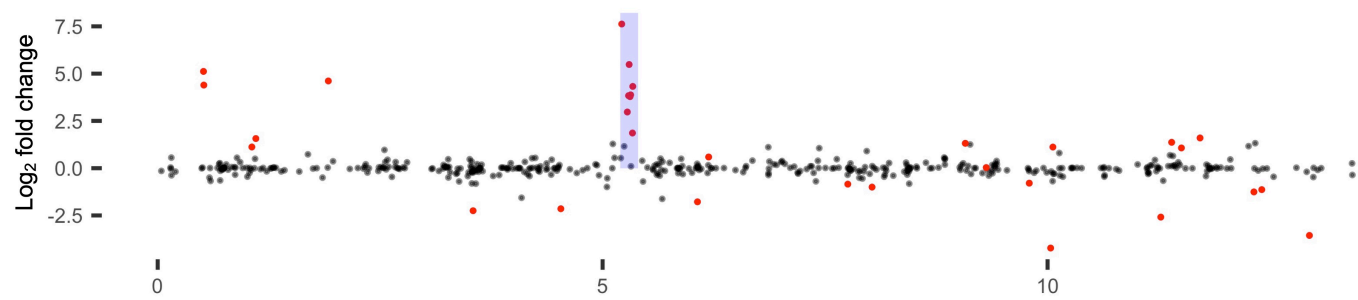




A



B



C

